Supporting Information

Stimuli-Responsive Anion Transport through Acylhydrazone-Based Synthetic Anionophores

Manzoor Ahmad,[a] Sandip Chattopadhayay,[a] Debashis Mondal,[a] Thangavel Vijayakanth,[b] and Pinaki Talukdar*,[a]

[a] Chemistry Department, Indian Institute of Science Education and Research Pune, Dr. Homi Bhabha Road, Pashan, Pune 411008, Maharashtra (India)

E-mail: ptalukdar@iiserpune.ac.in

Table of Contents

I. General Methods

All chemical reactions were performed under the nitrogen atmosphere. All reagents and solvents for synthesis were purchased from commercial sources (Sigma-Aldrich, Spectrochem) and used further without purification. The column chromatography was carried out using Merck silica (100-200 / 230-400 mesh size). The thin-layer chromatography was performed on E. Merck silica gel 60-F_{254} plates. Egg yolk phosphatidylcholine (EYPC) as a solution of chloroform (25 mg/mL), mini extruder, polycarbonate membrane of 100 nm and

200 nm were purchased from Avanti Polar Lipid. HEPES, HPTS, lucigenin, NaOH, Triton X-100, valinomycin, and all inorganic salts were obtained as molecular biology grade chemicals from Sigma Aldrich.

II. Physical Measurements

The ^{1}H NMR spectra were recorded at 400 MHz, whereas ^{13}C spectra at 101 MHz. The residual solvent signals were considered as an internal reference (δ_H = 7.26 ppm for $CDCl_3$, δ_H = 2.50 for DMSO-*d*$_6$, and δ_H = 1.94 for CD_3CN) to calibrate spectra. The chemical shifts were reported in ppm. Following abbreviations were used to indicate multiplicity patterns m: multiplet, s: singlet, d: doublet, t: triplet, q: quartet, p: pentet, dd: doublet of doublets, td: triplet of doublets. Coupling constants were measured in Hz. Infra-red (IR) spectra were measured in cm^{-1} using FT–IR spectrophotometer. Melting points were measured on a micro melting point apparatus. High-resolution mass spectra (HRMS) were recorded on electrospray ionization time-of-flight (ESI-TOF). Fluorescence experiments were recorded on Fluoromax-4 from Jobin Yvon Edison spectrometer equipped with an injector port, a microfluorescence cuvette holder, and a magnetic stirrer. All buffer solutions were prepared from the autoclaved water. Adjustment of pH of buffer solutions was made using the Helmer pH meter. The extravesicular dye was removed by performing gel chromatography using Sephadex G-50 resin. The fluorescence studies were proceed using OriginPro 8.5. ChemDraw 19 software was used for drawing structures and processing figures. UV-vis spectra were recorded on a Varian Cary 5000 spectrophotometer. The single-crystal X-ray diffraction (SCXRD) analysis was performed on a Bruker Smart Apex Duo diffractometer using Mo Kα radiation (λ = 0.71073Å). The crystal structures were solved using intrinsic methods and then refined by full-matrix least-squares against F^2 using all data by using SHELXL-2014/7 built in the Apex-3 package.

III. Synthesis

Scheme S1: Synthetic scheme for the preparation of compounds **1a–1d**.

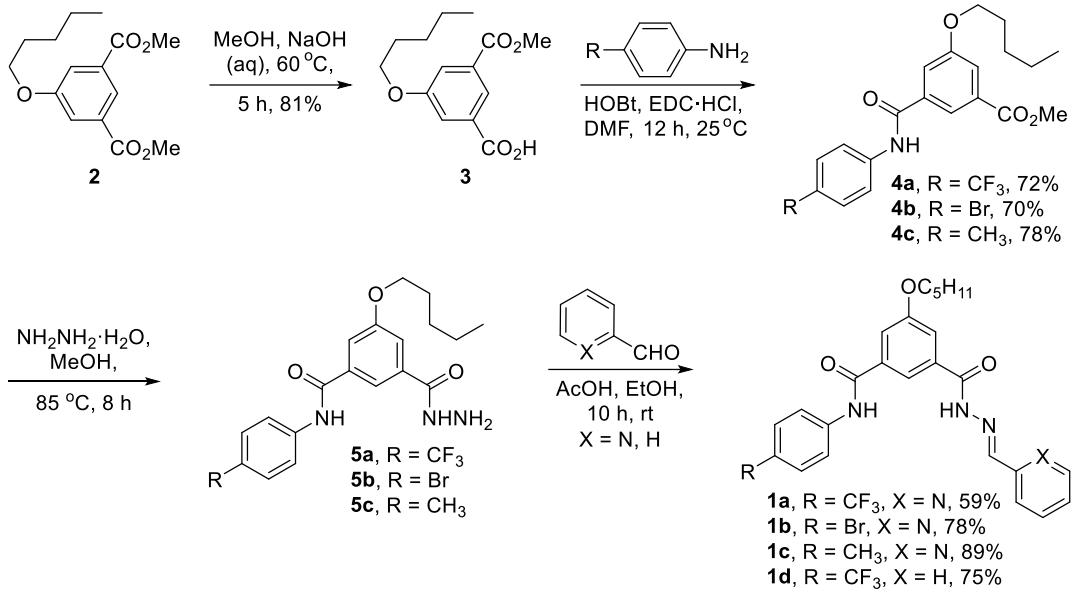

Synthetic Procedures

3-(Methoxycarbonyl)-5-(pentyloxy)benzoic acid, $C_{14}H_{18}O_5$ (3): A solution of **2** (2.0 g, 7.13 mmol) and NaOH (260 mg, 6.49 mmol) in MeOH (150 mL) and H_2O (25 mL) was heated under reflux conditions using an oil bath for 5 h. After cooling to the room temperature, the reaction mixture was poured into the cold water (60 mL) and the pH of the solution was adjusted to 1.0 using concentrated HCl. The reaction mixture was then extracted with ethyl acetate (2 x 50 mL), washed with brine and dried over Na_2SO_4. The solvant was evaoprated under reduced pressure and the crude mixture was purified by column chromatography over 100–200 mesh silica gel (*Eluent*: 1% MeOH in $CHCl_3$), to furnish the compound **3** as white solid (1.41 g, 81%). **M.P.:** 198.0–200 ˚C; **^{1}H NMR (400 MHz, $CDCl_3$):** δ 8.33 (s, 1H), 7.79 (s, 2H), 4.04 (t, *J* = 6.4 Hz, 2H), 3.94 (s, 3H), 1.82 (p, *J* = 6.5 Hz, 2H), 1.50 – 1.35 (m, 4H), 0.94 (t, *J* = 7.1 Hz, 3H); **^{13}C NMR (101 MHz, $CDCl_3$):** δ 170.9, 166.1, 159.3, 131.8, 130.7, 123.3, 120.6, 120.2, 68.6, 52.4, 28.7, 28.1, 22.4, 14.0; **IR (Neat, ν/cm^{-1}):** 3726, 3262, 3014, 2962, 2230, 1738, 1656, 1588, 1216, 1099; **HRMS (ESI) *m/z*:** $[M+H]^+$ Calcd. for $C_{14}H_{18}O_5H^+$ 267.1227; Found 267.1234.

General procedure for synthesizing amide derivatives (4a–4c)

In a 25 mL round bottom flask 3-(Methoxycarbonyl)-5-(pentyloxy)benzoic acid **3** (150 mg, 1 equiv.), EDC·HCl (128 mg, 0.4 mmol, 1.2 equiv.), and HOBt (54 mg, 0.4 mmol, 1.2 equiv.) were dissolved in DMF (10 mL). The resulted solution was stirred at room temperature for 30 min. After 30 min, *para*-substituted aniline derivatives (1 equiv.) and *N*, *N*-diisopropylethylamine (65 mg, 1.5 equiv.) were added. The reaction mixture was stirred at room temperature for an additional 12 h. After completion of the reaction, the reaction mixture was quenched with water (10 mL), extracted with ethyl acetate (3 × 20 mL) and washed with brine (2 × 20 mL). The combined organic layer was dried over Na_2SO_4 and concentrated under reduced pressure. The crude mixture was purified by column chromatography over 100–200 mesh silica gel to give pure **4a–4c**.

Methyl-3-(pentyloxy)-5-((4-(trifluoromethyl)phenyl)carbamoyl)benzoate, $C_{21}H_{22}F_3NO_4$ (4a): 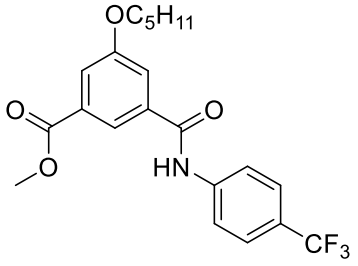

The crude product was purified by column chromotography (*Eluent*: EtOAc:petroleum ether 1:10 v/v), to furnish **4a** as white solid (165 mg, 72%). **M.P.:** 184.0–2186 ˚C; **^{1}H NMR (400 MHz, $CDCl_3$):** δ 8.05 (s, 1H), 8.02 (t, *J* = 1.4 Hz, 1H), 7.80 (d, *J* = 8.5 Hz, 2H), 7.74 (dd, *J* = 2.6, 1.3 Hz, 1H), 7.68 – 7.65 (m, 2H), 7.63 (s, 1H), 4.06 (t, *J* = 6.5 Hz, 2H), 3.96 (s, 3H), 1.88 – 1.77 (m, 2H), 1.51 – 1.34 (m, 4H), 0.94 (t, *J* = 7.2 Hz, 3H); **^{13}C NMR (101 MHz, $CDCl_3$):** δ 166.2, 164.8, 159.8, 140.8, 135.9, 131.9, 126.4, 126.4, 119.9, 119.2, 119.1, 118.3, 68.7, 52.6, 28.8, 28.1, 22.4, 14.1, 128–122 (qt); **IR (Neat, v/cm^{-1}):** 3726, 3262, 3014, 2962, 2230, 1738, 1656, 1588, 1216, 1099; **HRMS (ESI) *m/z*:** $[M+H]^+$ Calcd. for $C_{21}H_{22}F_3NO_4H^+$ 410.1574; Found 410.1578.

Methyl-3-((4-bromophenyl) carbamoyl)-5-(pentyloxy)benzoate, $C_{20}H_{22}BrNO_4$ (4b): 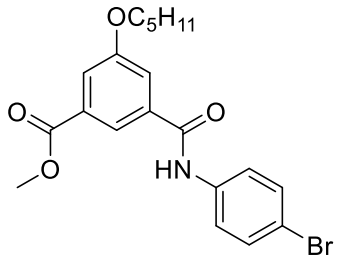

The crude product was purified by column chromotography (*Eluent*: EtOAc:petroleum ether 1:8 v/v), to furnish **4b** as white solid (163 mg, 70%). **M.P.:** 225.0–227 ˚C; **^{1}H NMR (400 MHz, $CDCl_3$):** δ 8.12 (s, 1H), 7.97 (t, *J* = 1.4 Hz, 1H), 7.67 (dd, *J* = 2.6, 1.3 Hz, 1H), 7.62 – 7.60 (m, 1H), 7.57 (d, *J* = 8.8 Hz, 2H), 7.47 (d, *J* = 8.8 Hz, 2H), 4.01 (t, *J* = 6.5 Hz, 2H), 3.92 (s, 3H), 1.80 (p, *J* = 6.6 Hz, 2H), 1.46 – 1.36 (m, 4H), 0.93 (t, *J* = 7.1 Hz, 3H); **^{13}C NMR (101 MHz, $CDCl_3$):** δ 166.2, 164.7, 159.7, 136.9, 136.2, 132.1, 131.7, 121.9, 119.2, 118.9, 118.3, 117.4,

68.7, 52.6, 28.8, 28.1, 22.4, 14.1; **IR (Neat, ν/cm^{-1}):** 3726, 3262, 3014, 2962, 2230, 1738, 1656, 1588, 1216, 1099; **HRMS (ESI) *m/z*:** $[M+H]^+$ Calcd. for $C_{20}H_{22}BrNO_4H^+$ 420.0805; Found 420.0798.

Methyl 3-(pentyloxy)-5-(*p*-tolylcarbamoyl) benzoate, $C_{21}H_{25}NO_4$ (4c): The crude product

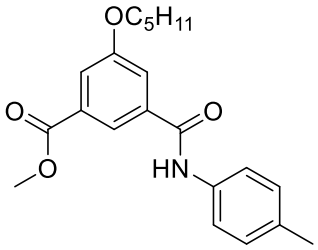

was purified by column chromotography (*Eluent*: EtOAc:petroleum ether 1:10 v/v), to furnish **4c** as white solid (156 mg, 78%); **M.P.:** 236–238 ˚C; **^{1}H NMR (400 MHz, $CDCl_3$):** δ 8.00 (t, *J* = 1.4 Hz, 1H), 7.88 (s, 1H), 7.70 (dd, *J* = 2.6, 1.3 Hz, 1H), 7.66 (dd, *J* = 2.4, 1.7 Hz, 1H), 7.53 (d, *J* = 8.4 Hz, 2H), 7.18 (d, *J* = 8.3 Hz, 2H), 4.05 (t, *J* = 6.5 Hz, 2H), 3.95 (s, 3H), 2.35 (s, 3H), 1.86 – 1.77 (m, 2H), 1.48 – 1.36 (m, 4H), 0.94 (t, *J* = 7.1 Hz, 3H); **^{13}C NMR (101 MHz, $CDCl_3$):** δ 166.3, 164.5, 159.7, 136.6, 135.1, 134.5, 131.8, 129.7, 120.4, 119.1, 118.7, 118.3, 68.7, 52.5, 28.8, 28.1, 22.4, 21.0, 14.1; **IR (Neat, ν/cm^{-1}):** 3726, 3262, 3014, 2962, 2230, 1738, 1656, 1588, 1216, 1099; **HRMS (ESI) *m/z*:** $[M+H]^+$ Calcd. for $C_{21}H_{25}NO_4H^+$ 356.1856; Found 356.1859.

3-(Hydrazinecarbonyl)-5-(pentyloxy)-*N*-(4-(bromo)phenyl)benzamide (5a): In a 25 mL

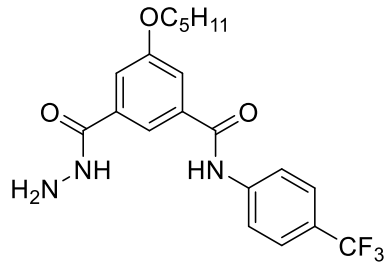

round bottom flask, **4a** (150 mg, 0.366 mmol, 1 equiv.) was dissolved in methanol (10 mL). Hydrazine monohydrate (356 µL, 7.33 mmol, 20 equiv.) was added, and the solution was refluxed at 60 °C using an oil bath for 8 h. After the completion of the reaction monitored through TLC, the solvent was evaporated under reduced pressure and the residue was extracted with ethyl acetate (2 × 20 mL), washed with brine solution, and dried over Na_2SO_4. The solvent was evaporated under reduced pressure and the crude product was used directly for the next reaction step without any further purification.

(*E*)-3-(pentyloxy)-5-(2-(pyridin-2-ylmethylene)hydrazine-1-carbonyl)-*N*-(4-

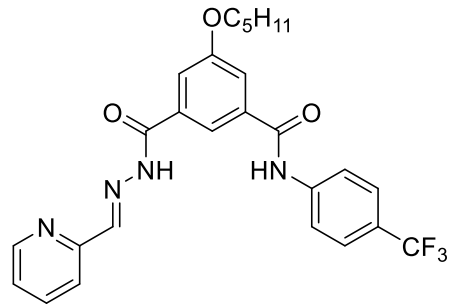

(trifluoromethyl)phenyl)benzamide, $C_{26}H_{25}F_3N_4O_3$ (1a): In a 20 mL round bottom flask, **5a** (150 mg, 0.366 mmol, 1 equiv.) was dissolved in absolute ethanol (6 mL). Picolinaldehyde (35 µL, 0.366 mmol, 1 equiv.) and acetic acid (2 mL) were added and the solution was

stirred at room temperature for 12 h. After the completion of the reaction, the solvent was removed under reduced pressure, extracted with ethyl acetate (3 × 20 mL), washed with brine solution and dried over Na_2SO_4. The crude reaction mixture was purified by column chromotography using 100–200 mesh silica gel (*Eluent*: 1% MeOH in CH_2Cl_2), to furnish the compound **1a** as white solid (111 mg, 59%). **M.P.:** 245–247 ˚C; **^{1}H NMR (400 MHz, DMSO-*d*$_6$):** δ 12.18 (s, 1H), 10.72 (s, 1H), 8.63 (d, *J* = 4.7 Hz, 1H), 8.51 (s, 1H), 8.11 (s, 1H), 8.02 (t, *J* = 9.7 Hz, 3H), 7.90 (t, *J* = 7.1 Hz, 1H), 7.75 (d, *J* = 8.7 Hz, 2H), 7.73 (s, 1H), 7.69 (s, 1H), 7.48 – 7.40 (m, 1H), 4.15 (t, *J* = 6.4 Hz, 2H), 1.79 (m, *J* = 6.6 Hz, 2H), 1.51 – 1.31 (m, 4H), 0.92 (t, *J* = 7.1 Hz, 3H); **^{13}C NMR (101 MHz, DMSO-*d*$_6$):** δ 165.6, 162.9, 159.1, 153.6, 150.0, 148.9, 143.0, 137.3, 136.6, 135.23, 126.3, 126.1 – 125.7 (m), 124.9, 124.4, 123.4, 120.6, 119.8, 117.3, 115.1, 68.6, 28.7, 28.1, 22.3, 14.3; **IR (Neat, ν/cm^{-1}):** 3726, 3262, 3014, 2962, 2230, 1738, 1656, 1588, 1216, 1099; **HRMS (ESI) *m/z*:** $[M+H]^+$ Calcd. for $C_{26}H_{25}F_3N_4O_3H^+$ 499.1952; Found 499.1957.

***N*-(4-Bromophenyl)-3-(hydrazinecarbonyl)-5-(pentyloxy)benzamide (5b):** In a 25 mL round bottom flask, **4b** (150 mg, 0.356 mmol, 1 equiv.) was dissolved in absolute methanol (10 mL). Hydrazine monohydrate (346 µL, 7.14 mmol, 20 equiv.) was added, and the solution was refluxed at 60 °C using an oil bath for 8 h. The completion of the reaction was monitored through TLC. Subsequently, the solvent was evaporated under reduced pressure. The residue was extracted with Ethyl acetate (2 × 20 mL), washed with brine solution, and dried over Na_2SO_4. The solvent was evaporated, and the crude product was used directly for the next step without any further purification.

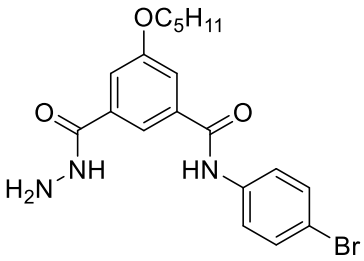

(*E*)-*N*-(4-bromophenyl)-3-(pentyloxy)-5-(2-(pyridin-2-ylmethylene)hydrazine carbonyl)benzamide, $C_{25}H_{25}BrN_4O_3$ (1b): In a 20 mL round bottom flask, **5b** (150 mg, 0.357 mmol, 1 equiv.) was dissolved in absolute ethanol (6 mL). Picolinaldehyde (34 µL, 0.357 mmol, 1 equiv.) and acetic acid (2 mL) were added and the solution was stirred at room temperature for 12 h. The solvent was removed under reduced pressure and the residue was extracted with ethyl acetate (3 × 20 mL), washed with brine and dried over Na_2SO_4. The crude reaction mixture was purified by column

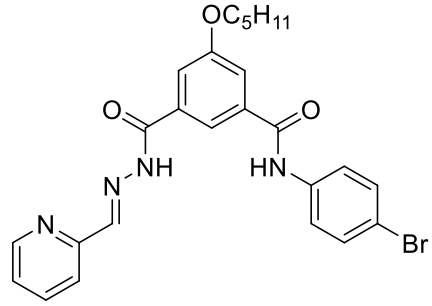

chromotography using 100–200 mesh silica gel (*Eluent*: 3% MeOH in CH_2Cl_2), to furnish the compound **1b** as white solid (142 mg, 78%). **M.P.:** 253–255 ˚C; **^{1}H NMR (400 MHz, DMSO-*d*$_6$):** δ 12.12 (s, 1H), 10.46 (s, 1H), 8.59 (d, *J* = 4.4 Hz, 1H), 8.47 (s, 1H), 8.05 (s, 1H), 7.96 (d, *J* = 7.9 Hz, 1H), 7.86 (t, *J* = 7.5 Hz, 1H), 7.74 (d, *J* = 8.8 Hz, 2H), 7.64 (d, *J* = 11.4 Hz, 2H), 7.52 (d, *J* = 8.8 Hz, 2H), 7.42 – 7.34 (m, 1H), 4.09 (t, *J* = 6.3 Hz, 2H), 1.73 (q, *J* = 6.6 Hz, 2H), 1.43–1.31 (m, 4H), 0.87 (t, *J* = 7.1 Hz, 3H); **^{13}C NMR (101 MHz, DMSO-*d*$_6$):** δ 165.2, 163.0, 159.2, 156.8, 153.7, 150.1, 149.0, 138.8, 137.4, 136.9, 135.2, 132.0, 125.0, 122.9, 120.5, 119.8, 117.1, 116.1, 68.7, 28.8, 28.2, 22.4, 14.4; **IR (Neat, ν/cm^{-1}):** 3726, 3262, 3014, 2962, 2230, 1738, 1656, 1588, 1216, 1099; **HRMS (ESI) *m/z*:** $[M+H]^+$ Calcd. for $C_{25}H_{25}BrN_4O_3H^+$ 509.1183; Found 509.1178.

3-(Hydrazinecarbonyl)-5-(pentyloxy)-*N*-(*p*-tolyl)benzamide (5c): In a 25 mL round bottom flask, **4c** (150 mg, 0.422 mmol, 1 equiv.) was dissolved in absolute methanol (10 mL). Hydrazine monohydrate (410 µL, 8.44 mmol, 20 equiv.) was added, and the solution was refluxed at 60 °C using an oil bath for 8 h. The completion of the reaction was monitored by TLC. Subsequently, the solvent was evaporated under reduced pressure. The residue was extracted with ethyl acetate (2 × 20 mL), washed with brine, and dried over Na_2SO_4. The solvent was evaporated and the crude product was used directly for the next step without any further purification.

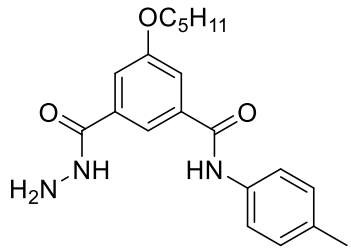

(*E*)-3-(pentyloxy)-5-(2-(pyridin-2-ylmethylene)hydrazine-1-carbonyl)-*N*-(*p*-tolyl)benzamide, $C_{26}H_{28}N_4O_3$ (1c): In a 25 mL round bottom flask, **5c** (150 mg, 0.422 mmol, 1 equiv.) was dissolved in absolute ethanol (6 mL). Picolinaldehyde (40 µL, 0.422 mmol, 1 equiv.) and acetic acid (2 mL) were added and the solution was stirred at room temperature for 12 h. After the completion of the reaction, the solvent was removed under reduced pressure and the residue was extracted with ethyl acetate (3 × 20 mL), washed with brine and dried over Na_2SO_4. The crude reaction mixture was purified by column chromatography using 100–200 mesh silica gel (*Eluent*: 1% MeOH in CH_2Cl_2), to furnish the compound **1c** as white solid (168 mg, 89%). **M.P.:** 236–238 ˚C; **^{1}H NMR (400 MHz, DMSO-*d*$_6$):** δ 12.15 (s, 1H), 10.30 (s, 1H), 8.63 (d, *J* = 4.4 Hz, 1H), 8.51 (s, 1H), 8.09 (s, 1H), 8.00 (d, *J* = 7.9 Hz, 1H), 7.90 (t, *J* = 7.5 Hz, 1H), 7.69 (d, *J* = 9.0 Hz, 2H), 7.66 (s,

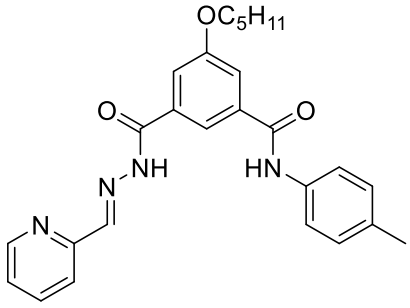

2H), 7.47 – 7.41 (m, 1H), 7.19 (s, 1H), 7.16 (s, 1H), 4.14 (t, *J* = 6.3 Hz, 2H), 2.28 (s, 3H), 1.78 (q, *J* = 6.6 Hz, 2H), 1.42 (ddd, *J* = 27.0, 14.8, 7.5 Hz, 4H), 0.92 (t, *J* = 7.1 Hz, 3H); **^{13}C NMR (101 MHz, DMSO-*d*$_6$):** δ 164.9, 163.0, 159.1, 153.7, 150.1, 148.9, 137.4, 137.2, 136.9, 135.1, 133.3, 129.5, 125.0, 121.0, 120.5, 119.7, 117.2, 116.9, 68.6, 28.8, 28.2, 22.4, 21.0, 14.5; **IR (Neat, ν/cm^{-1}):** 3726, 3262, 3014, 2962, 2230, 1738, 1656, 1588, 1216, 1099; **HRMS (ESI) *m/z*:** $[M+H]^+$ Calcd. for $C_{26}H_{28}N_4O_3H^+$ 445.2234; Found 445.2238.

(*E*)-3-(2-benzylidenehydrazine-1-carbonyl)-5-(pentyloxy)-N-(4-(trifluoromethyl) phenyl)benzamide, $C_{27}H_{26}F_3N_3O_3$ (1d): In a 25 mL round bottom flask, **5a** (150 mg, 0.422 mmol, 1 equiv.) was dissolved in absolute ethanol (6 mL). Benzaldehyde (40 µL, 0.422 mmol, 1 equiv.) and acetic acid (2 mL) were added and the solution was stirred at room temperature for 12 h. After the completion of the reaction, the solvent was removed under reduced pressure and the residue was extracted with ethyl acetate (3 × 20 mL), washed with brine and dried over Na_2SO_4. The crude reaction mixture was purified by column chromotography using 100–200 mesh silica gel (*Eluent*: 1% MeOH in CH_2Cl_2), to furnish the compound **1d** as white solid (138 mg, 75%). **M.P.:** 212–214 ˚C; **^{1}H NMR (400 MHz, DMSO-*d*$_6$):** δ 11.98 (s, 1H), 10.71 (s, 1H), 8.49 (s, 1H), 8.10 (s, 1H), 8.03 (d, *J* = 8.5 Hz, 2H), 7.75 (d, *J* = 8.2 Hz, 4H), 7.69 (d, *J* = 12.0 Hz, 2H), 7.47 (q, *J* = 4.8 Hz, 3H), 4.14 (t, *J* = 6.4 Hz, 2H), 1.79 (p, *J* = 6.6 Hz, 2H), 1.50 – 1.32 (m, 4H), 0.92 (t, *J* = 7.1 Hz, 3H); **^{13}C NMR (101 MHz, DMSO-*d*$_6$):** δ 162.6, 159.1, 148.7, 143.1, 136.6, 135.4, 134.7, 130.7, 129.3, 127.6, 126.4, 126.1, 124.7–123.8 (q), 123.4, 120.7, 119.8, 117.3, 117.1, 68.6, 28.8, 28.1, 22.3, 14.4; **IR (Neat, ν/cm^{-1}):** 3726, 3262, 3014, 2962, 2230, 1738, 1656, 1588, 1216, 1099; **HRMS (ESI) *m/z*:** $[M+H]^+$ Calcd. for $C_{26}H_{25}F_3N_4O_3H^+$ 499.1952; Found 499.1957.

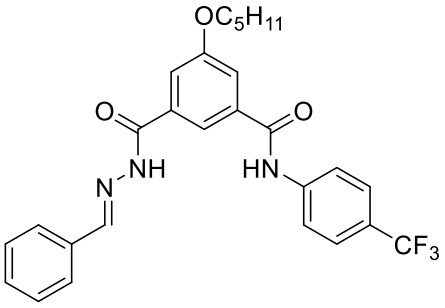

IV. Anion Binding Studies

^{1}H NMR titration was carried out at room temperature on Bruker 400 MHz spectrometer. The residual solvent signal (CD_3CN, δ_H = 1.94) was considered as an internal reference to calibrate spectra. TBACl, TBABr, TBAI and $TBAClO_4$ salt, and receptor were dried under a high vacuum before use. The titrations were performed by the addition of aliquots from either solution of TBACl, TBABr, TBAI and $TBAClO_4$ (0.5M in CD_3CN) to the solution of receptors **1a**, **1b**, **1c**, **1d**, and **1a-*Z*** (i.e., the photoisomerized sample of **1a**) (0.005 M in

CD_3CN). All NMR data were processed using MestReNova 6.0 and collected data was fitted in a different binding mode using BindFit v0.5.[S1]

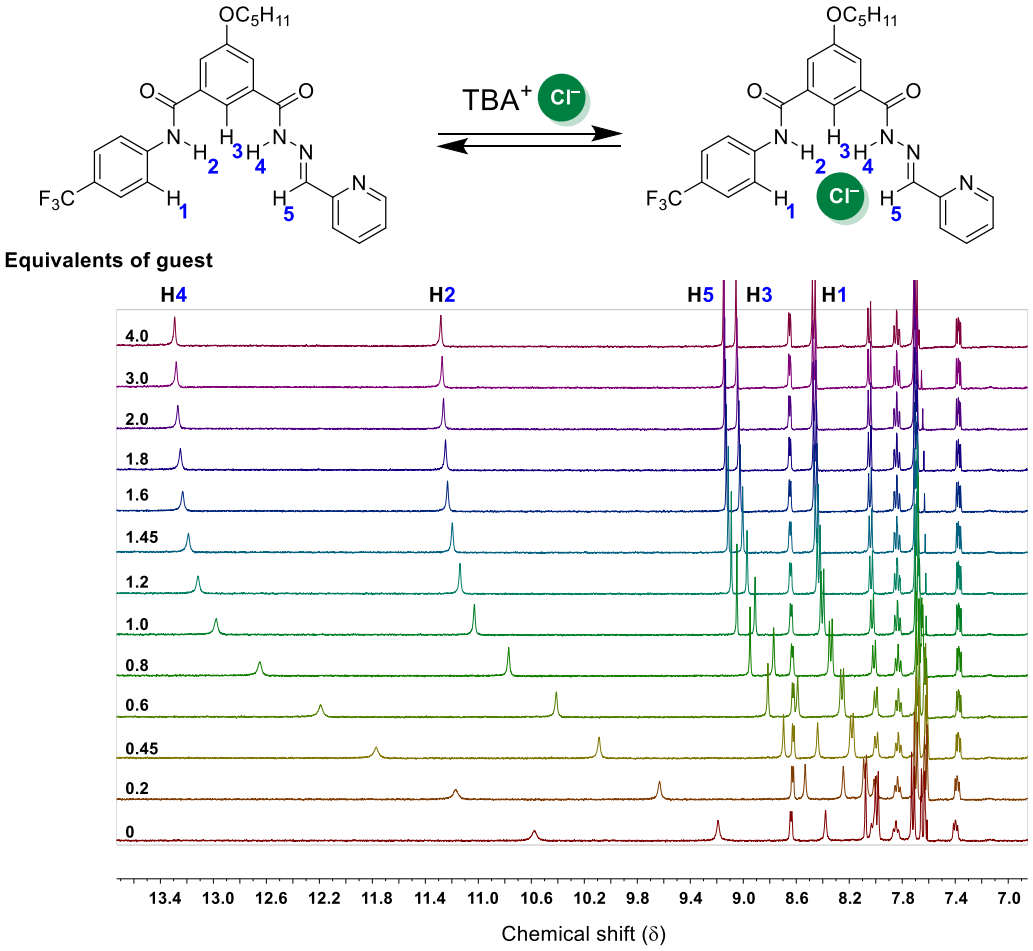

Figure S1. ^1H NMR titration spectra for **1a** (5 mM) with stepwise addition of TBACl in CD_3CN. The equivalents of added TBACl are shown on the stack spectra.

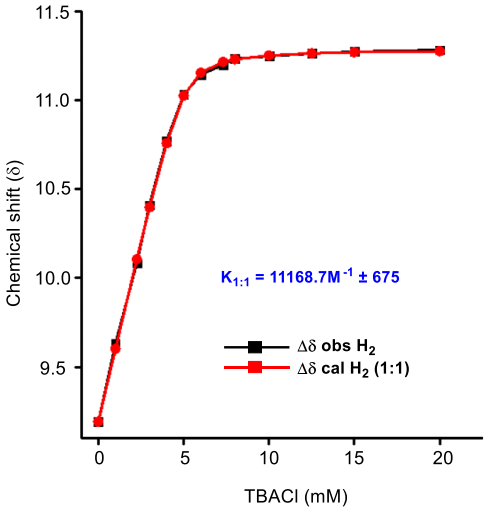

Figure S2. The plot of chemical shift (δ) of H_2 protons *vs* concentration of TBACl added, fitted to 1:1 binding model of BindFit v0.5. The binding constant obtained is the mean of the three independent experiments.

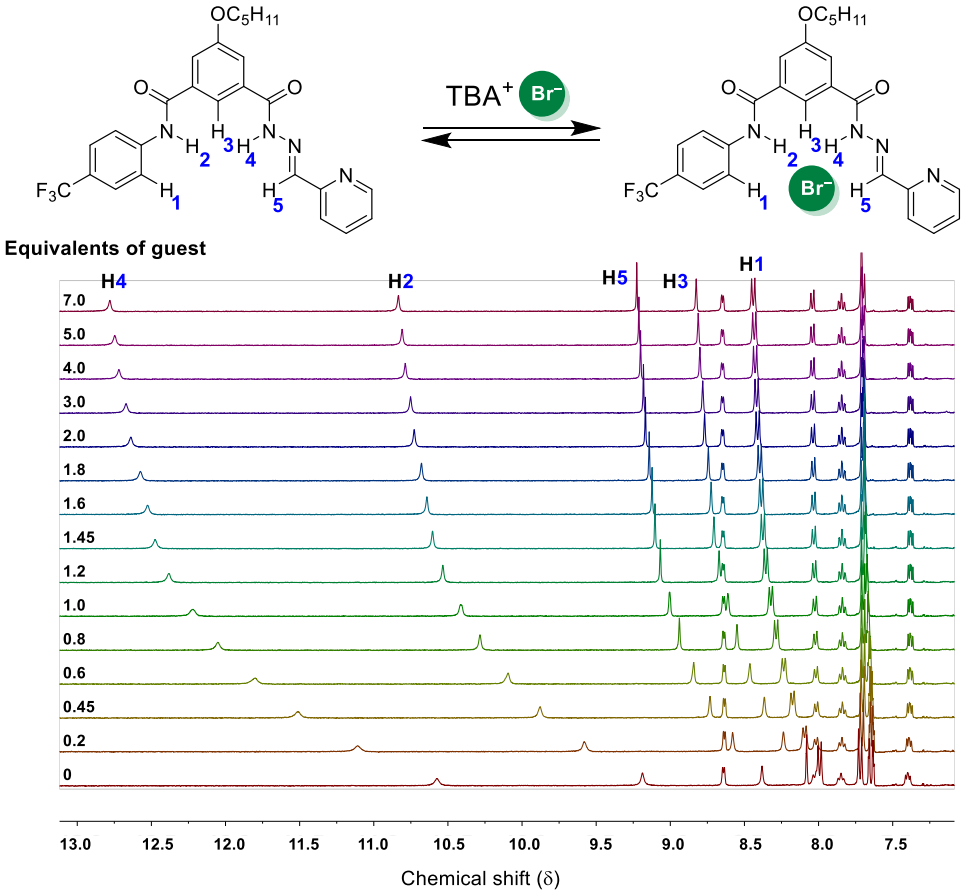

Figure S3. ^{1}H NMR titration spectra for **1a** (5 mM) with stepwise addition of TBABr in CD_3CN. The equivalents of added TBABr are shown on the stack spectra.

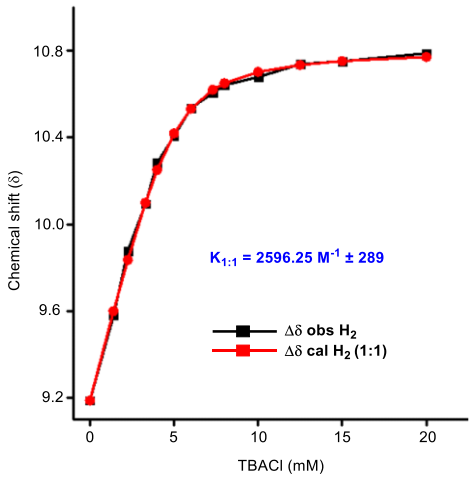

Figure S4. The plot of chemical shift (δ) of H_2 protons *vs* concentration of TBABr added, fitted to 1:1 binding model of BindFit v0.5. The binding constant obtained is the mean of the three independent experiments.

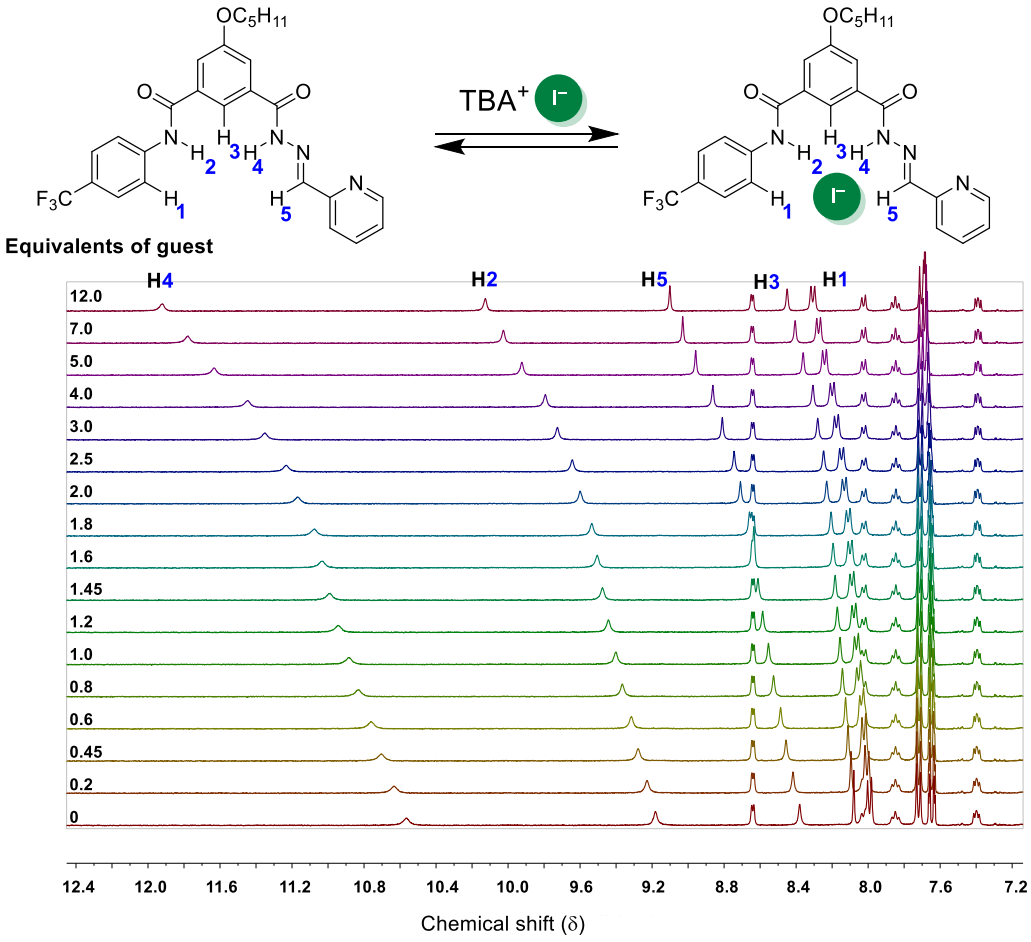

Figure S5. ^{1}H NMR titration spectra for **1a** (5 mM) with stepwise addition of TBAI in CD_3CN. The equivalents of added TBAI are shown on the stack spectra.

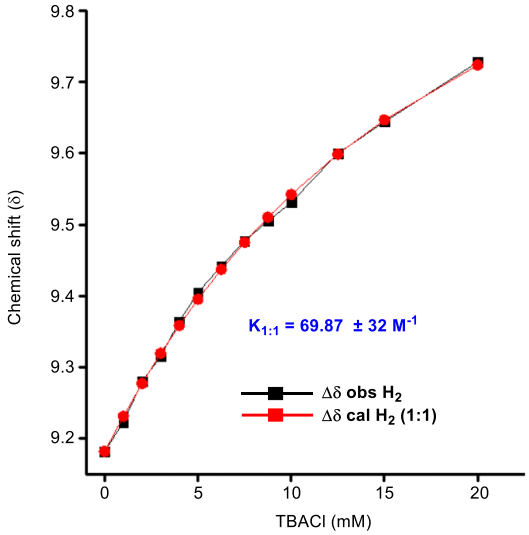

Figure S6. The plot of chemical shift (δ) of H_2 protons *vs* concentration of TBAI added, fitted to 1:1 binding model of BindFit v0.5. The binding constant obtained is the mean of the three independent experiments.

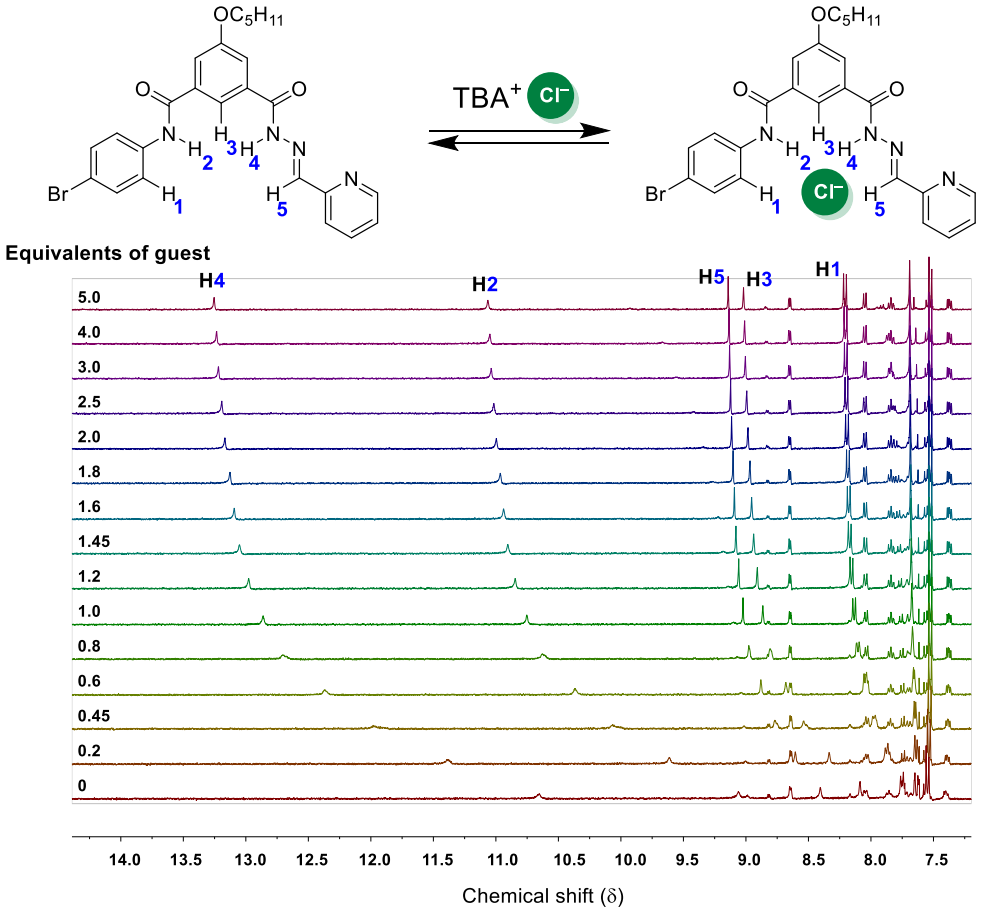

Figure S7. ^{1}H NMR titration spectra for **1b** (5 mM) with stepwise addition of TBACl in CD_3CN. The equivalents of added TBACl are shown on the stack spectra.

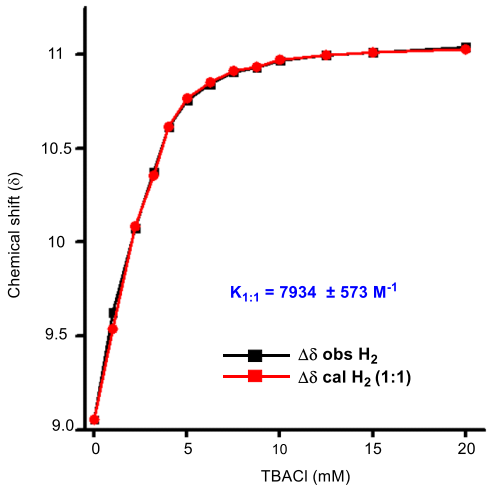

Figure S8. The plot of chemical shift (δ) of H_2 protons *vs* concentration of TBACl added, fitted to 1:1 binding model of BindFit v0.5. The binding constant obtained is the mean of the three independent experiments.

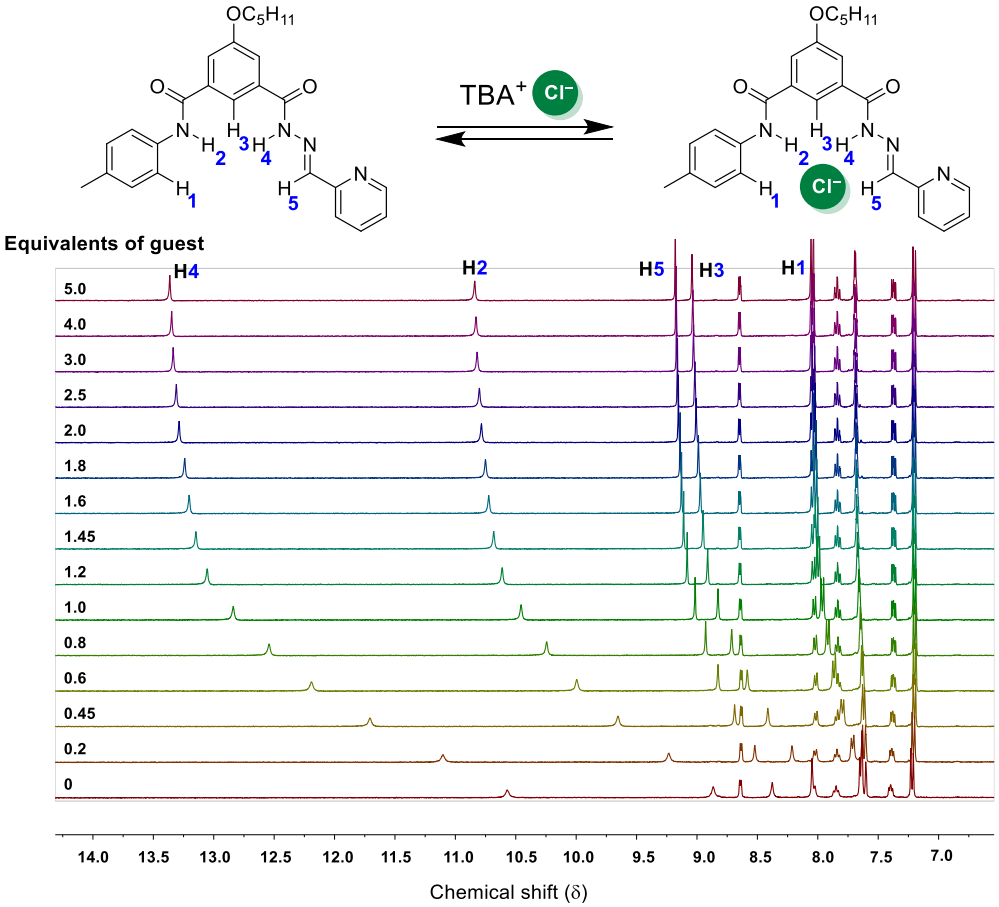

Figure S9. ^{1}H NMR titration spectra for **1c** (5 mM) with stepwise addition of TBACl in CD_3CN. The equivalents of added TBACl are shown on the stack spectra.

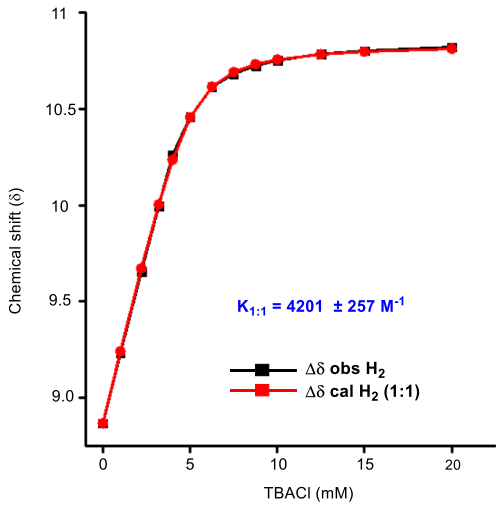

Figure S10. The plot of chemical shift (δ) of H_2 protons *vs* concentration of TBACl added, fitted to 1:1 binding model of BindFit v0.5. The binding constant obtained is the mean of the three independent experiments.

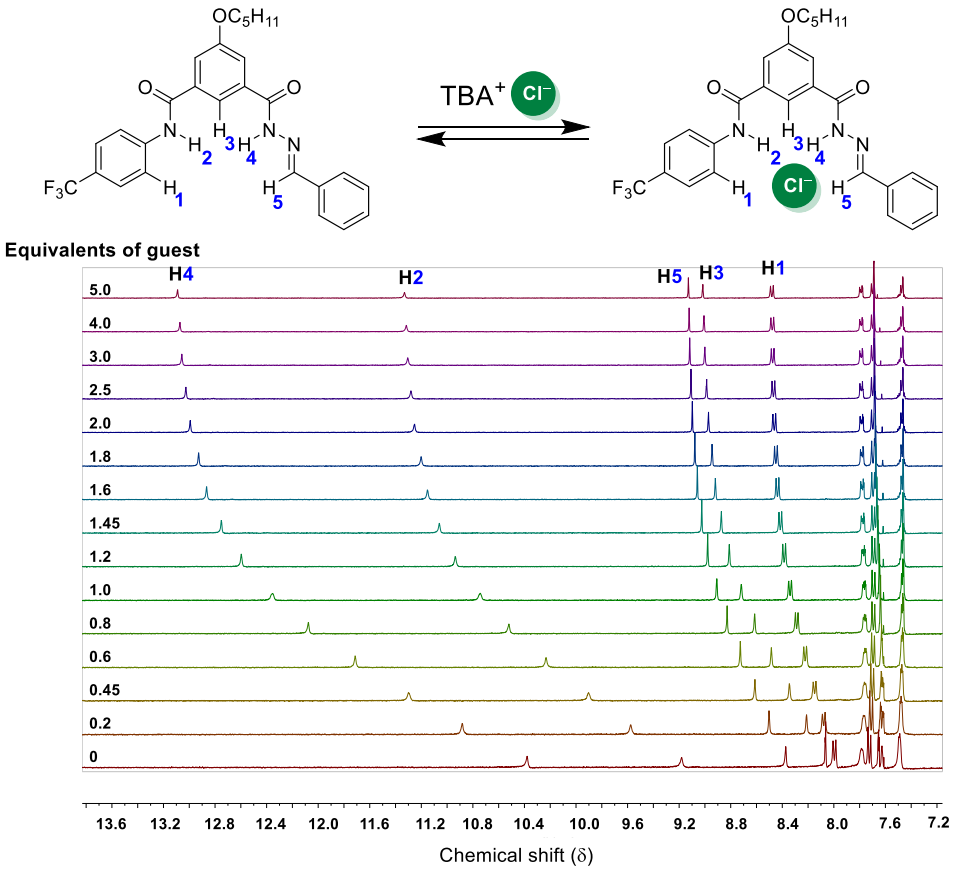

Figure S11. ^{1}H NMR titration spectra for **1d** (5 mM) with stepwise addition of TBACl in CD_3CN. The equivalents of added TBACl are shown on the stack spectra.

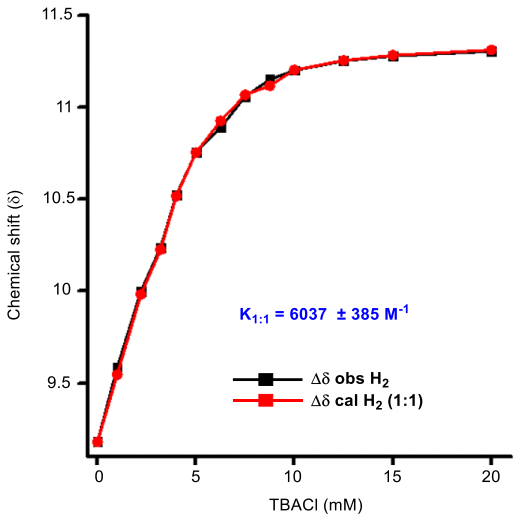

Figure S12. The plot of chemical shift (δ) of H_2 protons *vs* concentration of TBACl added, fitted to 1:1 binding model of BindFit v0.5. The binding constant obtained is the mean of the three independent experiments.

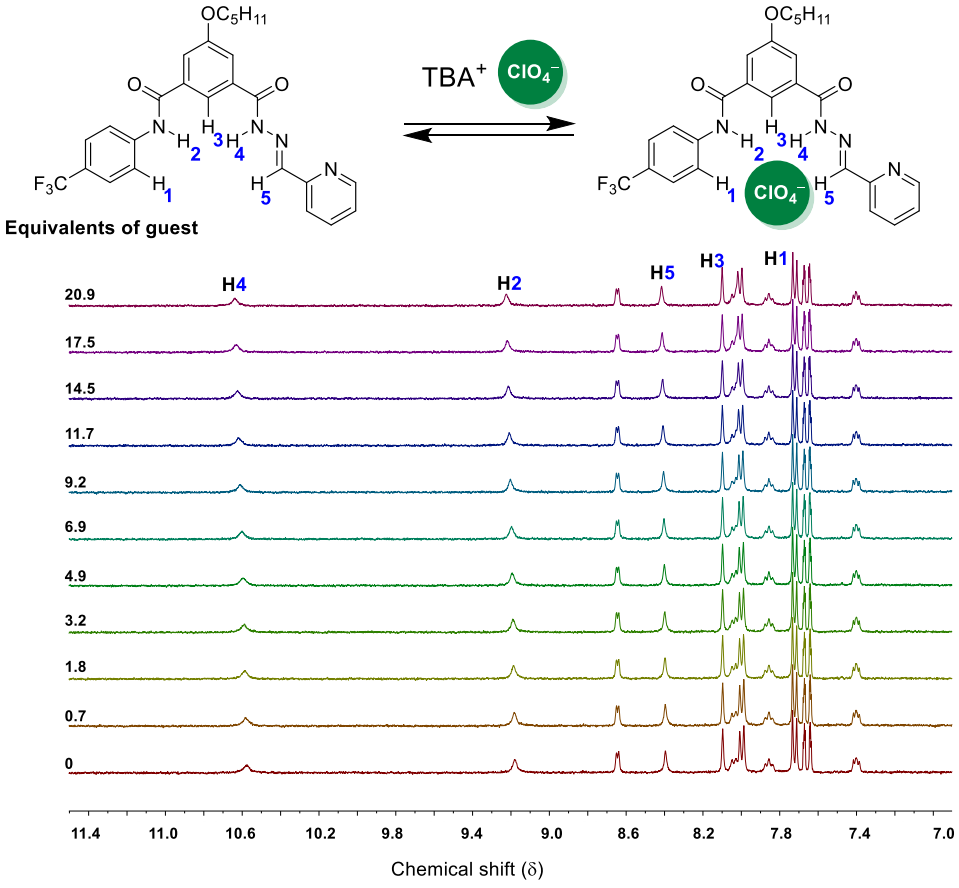

Figure S13. ^{1}H NMR titration spectra for **1a** (5 mM) with stepwise addition of $TBAClO_4$ in CD_3CN. The equivalents of added $TBAClO_4$ are shown on the stack spectra.

^{1}H NMR titration studies for 1a-*Z*

To get the binding affinity for **1a–*Z***, a solution of **1a–*E*** (i.e. the as-synthesized compound) (10 mg) in acetonitrile was photoirradiated at 312 nm using UV tubes (8W × 3) for 30 min. The photoirradiated sample was dried and then purified by column chromatography (Eluent: 1% MeOH in CH_2Cl_2) to get the pure **1a–*Z***. The pure **1a–*Z*** was used for the ^{1}H NMR binding studies with TBACl (Figure S14).

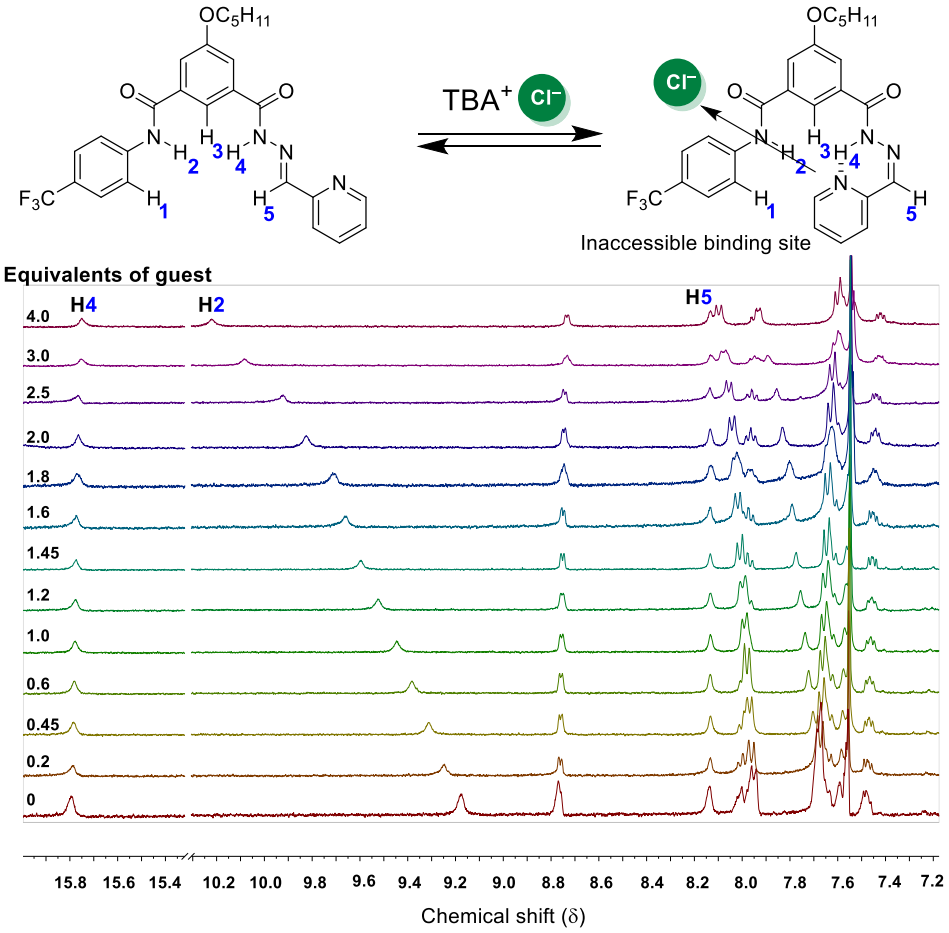

Figure S14. ^{1}H NMR titration spectra for **1a–*Z*** (5 mM) with stepwise addition of TBACl in CD_3CN. The equivalents of added TBACl are shown on the stack spectra.

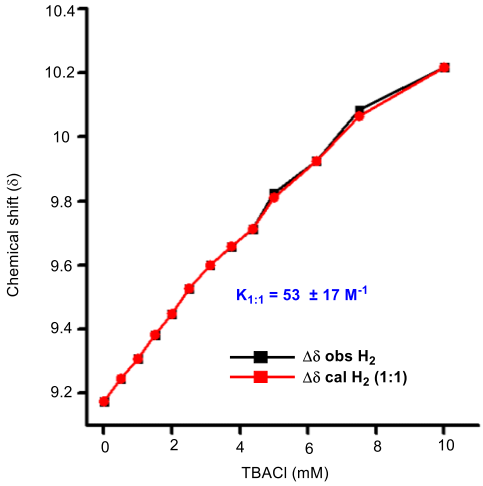

Figure S15. The plot of chemical shift (δ) of H_2 protons *vs* concentration of TBACl added, fitted to 1:1 binding model of BindFit v0.5. The binding constant obtained is the mean of the three independent experiments.

Table S1. ^{1}H NMR titration studies of compounds **1a**–**1d** with different salts of TBACl, TBABr, TBAI and $TBAClO_4$ salts in acetonitrile-d_3, and **1a**–*Z* with TBACl.

Association constant, $K_a \times 10^3$ (M^{-1}) in CD_3CN				
Comp.	Cl^-	Br^-	I^-	ClO_4^-
1a–*E*	11.16 ± 675	2.59 ± 289	0.069 ± 17	– [b]
1b	7.9 ± 573	– [a]	– [a]	– [a]
1c	4.2 ± 257	– [a]	– [a]	– [a]
1d	6.02 ± 385	– [a]	– [a]	– [a]
1a–*Z*	0.053 ± 11	– [a]	– [a]	– [a]

[a] = ^{1}H NMR titration was not done with these systems, and [b] = Binding constant could not be determined due to the absence of any chemical shift in ^{1}H NMR titration of **1a** with ClO_4^-.

V. Mass Spectrometric Studies

Stock solutions of **1a** and TMACl (Tetramethyl ammonium chloride) (1 mM each) were prepared in spectroscopy grade CH_3CN. Solutions were mixed in equal proportion and diluted to get 10 μM concentrations of each species in CH_3CN. Sample was electrosprayed at a flow rate of 5.0 μL/min. A constant spray and highest intensities were achieved with a capillary voltage of 2500 V at a source temperature of 80 °C. The parameters for sample cone (20 V) and extractor cone voltage (5 V) were optimized for maximum intensities of the

desired complexes. Figure S16 represents the ESI-MS data recorded from CH_3CN solution of **1a** with TMACl prepared in 1:1 molar ratio.

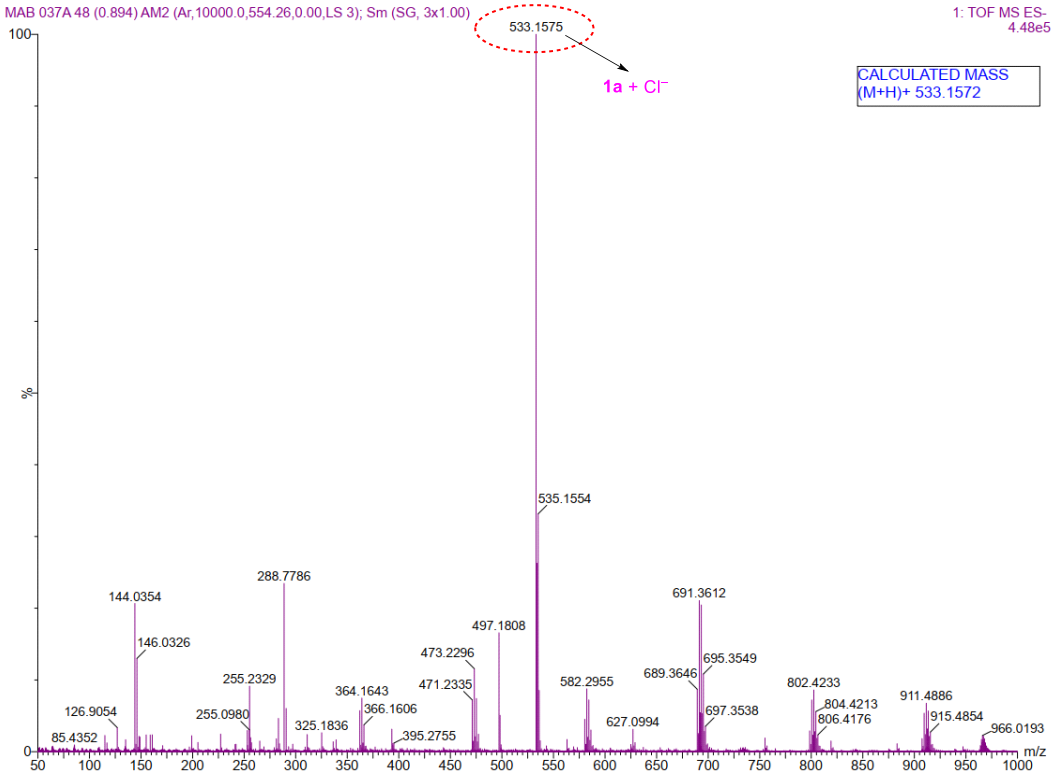

Figure S16. Complete (*m/z* = 50 to 1000) of ESI-MS spectrum of 1:1 mixture of **1a** and TMACl recorded in CH_3CN.

VI. Ion Transport Studies[S2]

A. Ion transporting activity studies across EYPC-LUVs⊃HPTS

Preparation of HEPES buffer and stock solutions: The HEPES buffer of pH = 7.0 was prepared by dissolving an appropriate amount of solid HEPES (10 mM) and NaCl (100 mM) in autoclaved water. The pH was adjusted to 7.0 by addition aliquots from 0.5 M NaOH solution. The stock solution of all carriers was prepared using HPLC grade DMSO.

Preparation of EYPC-LUVs⊃HPTS in NaCl: In 10 mL clean and dry round bottom flask, a thin transparent film of egg yolk phosphatidylcholine (EYPC) was formed using a 1 mL EYPC lipid (25 mg/mL in $CHCl_3$) by providing continuous rotation and purging nitrogen gas. The transparent thin film was completely dried under a high vacuum for 4-5 h. After that, the transparent thin film was hydrated with 1 mL HEPES buffer (1 mM HPTS, 10 mM HEPES, 100 mM NaCl, pH = 7.0) and the resulting suspension was vortexed at 10 min intervals during 1 h. This hydrated suspension was subjected to 15 cycles of freeze-thaw (liquid

nitrogen, 55 °C) followed by extrusion through 100 nm (pore size) polycarbonate membrane for 21 times to obtain the vesicles of an average 100 nm diameter. The unentrapped HPTS dyes were removed by size exclusion chromatography using Sephadex G-50 and eluting with HEPES buffer (10 mM HEPES, 100 mM NaCl, pH = 7.0). Finally, collected vesicles were diluted to 6 mL to get EYPC-LUVs⊃HPTS. *Final conditions:* ~ 5 mM EYPC, Inside: 1 mM HPTS, 10 mM HEPES, 100 mM NaCl, pH = 7.0, Outside: 10 mM HEPES, 100 mM NaCl, pH = 7.0.

Ion transport activity by HPTS assay: In clean and dry fluorescence cuvette, 1975 μL of HEPES buffer (10 mM HEPES, 100 mM NaCl, pH =7.0) and 25 μL of EYPC–LUVs⊃HPTS vesicle was added. The cuvette was placed in slowly stirring condition using a magnetic stirrer equipped within a fluorescence instrument ($t = 0$ s). The time-dependent HPTS emission intensity monitored at λ_{em} = 510 nm (λ_{ex} = 450 nm) by creating pH gradient between intra- and extra- vesicular system by adding 0.5 M NaOH (20 μL) at t = 20 s. Then different concentrations of transporter molecules in DMSO were added at t = 100 s. Finally, the vesicles were lysed by addition of 10% Triton X-100 (25 μL) at t = 300 s to disturbed pH gradient.

The time axis was normalized according to Equation S1:

$$t = t - 100 \qquad \text{Equation S1}$$

The time-dependent data were normalized to percent change in fluorescence intensity using Equation S2:

$$I_F = [(I_t - I_0) / (I_\infty - I_0)] \times 100 \qquad \text{Equation S2}$$

where, I_0 is the initial intensity, I_t is the intensity at time t, and I_∞ is the final intensity after the addition of Triton X-100.

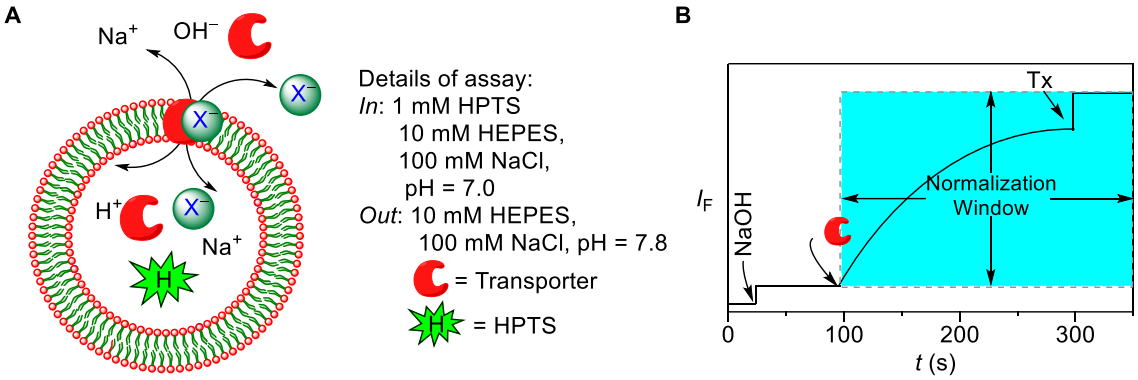

Figure S17. Representation of fluorescence-based ion transport assay using EYPC-LUVs⊃HPTS (A), and illustration of transport kinetics showing normalization window (B).

Dose-response activity: The fluorescence kinetics of each transporter at different concentration was studied as a course of time. The concentration profile data were evaluated at t = 290 s to get effective concentration, EC_{50} (i.e. the concentration of transporter needed to achieve 50% chloride efflux)[S3] using Hill equation (Equation S3):

$$Y = Y_\infty + (Y_0 - Y_\infty) / [1 + (c/EC_{50})^n] \qquad \text{Equation S3}$$

where, Y_0 = Fluorescence intensity just before the transporter addition (at t = 0 s), Y_∞ = Fluorescence intensity with excess transporter concentration, c = Concentration of transporter compound, and n = Hill coefficient (i.e. indicative for the number of monomers needed to form an active supramolecule).[S4]

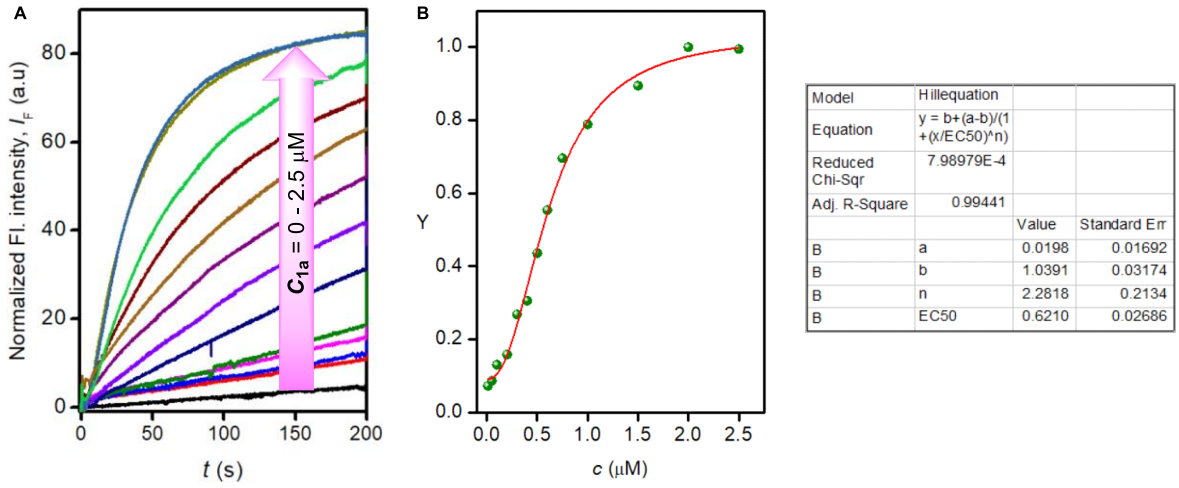

Model	Hillequation		
Equation	y = b+(a-b)/(1+(x/EC50)^n)		
Reduced Chi-Sqr	7.98979E-4		
Adj. R-Square	0.99441		
		Value	Standard Err
B	a	0.0198	0.01692
B	b	1.0391	0.03174
B	n	2.2818	0.2134
B	EC50	0.6210	0.02686

Figure S18. Concentration-dependent activity of **1a** across EYPC-LUVs⊃HPTS (A), and Hill plot of compound **1a** at t = 180 s to get EC_{50} and n (B).

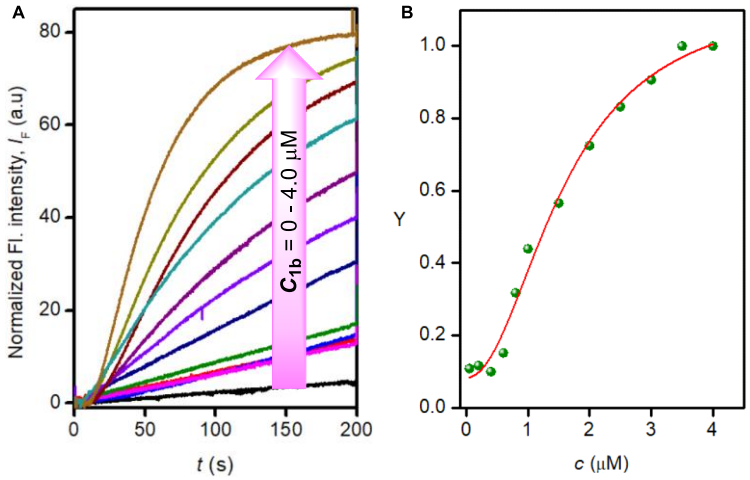

Model	Hillequation (User)		
Equation	y = b+(a-b)/(1 +(x/EC50)^n)		
Reduced Chi-Sqr	0.00197		
Adj. R-Square	0.98756		
		Value	Standard Erro
B	a	-0.05574	0.05228
B	b	1.19097	0.13341
B	n	1.91341	0.39068
B	EC50	1.58718	0.2009

Figure S19. Concentration-dependent activity of **1b** across EYPC-LUVs⊃HPTS (A), and Hill plot of compound **1b** at t = 180 s to get EC_{50} and n (B).

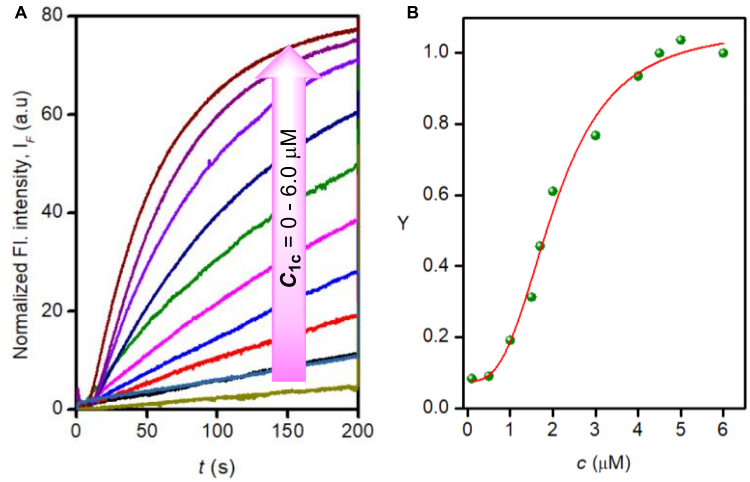

Model	Hillequation (User)		
Equation	y = b+(a-b)/(1+(x/EC50)^n)		
Reduced Chi-Sqr	0.00218		
Adj. R-Square	0.98615		
		Value	Standard Error
B	a	-0.01495	0.04437
B	b	1.09471	0.06952
B	n	2.78947	0.51351
B	EC50	2.08632	0.15223

Figure S20. Concentration-dependent activity of **1c** across EYPC-LUVs⊃HPTS (A), and Hill plot of compound **1c** at t = 180 s to get EC_{50} and n (B).

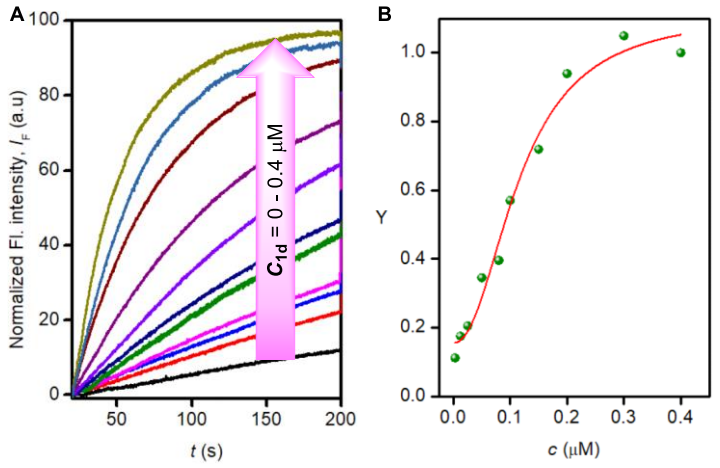

Model	Hillequation		
Equation	y = b+(a-b)/(1 +(x/EC50)^n)		
Reduced Chi-Sqr	0.00301		
Adj. R-Square	0.9764		
		Value	Standard Erro
C	a	0.15638	0.03691
C	b	1.11576	0.0893
C	n	2.15901	0.51282
C	EC50	0.11688	0.01453

Figure S21. Concentration-dependent activity of **1d** across EYPC-LUVs⊃HPTS (A), and Hill plot of compound **1d** at t = 180 s to get EC_{50} and n (B).

B. Chloride transport activity across EYPC-LUVs⊃lucigenin vesicles

Preparation of EYPC-LUVs⊃lucigenin vesicles: In 10 mL clean and dry round bottom flask, the thin transparent film of egg yolk phosphatidylcholine (EYPC) was formed by drying 1.0 mL egg yolk phosphatidylcholine (EYPC, 25 mg/mL in $CHCl_3$) with providing continuous rotation and purging nitrogen. The transparent thin film was kept under a high vacuum for 4 hours to remove all traces of $CHCl_3$. Then the transparent thin film was hydrated with 1.0 mL aqueous $NaNO_3$ (200 mM, 1.0 mM Lucigenin) with occasional vortexing at 10 min intervals for 1 h. The resulting suspension was subjected to freeze and thaw cycles (≥ 15, liquid nitrogen, 55 ^oC water bath) and 21 times extrusion through 200 nm pore size polycarbonate membrane. The size exclusion chromatography (using Sephadex G-50) was performed to remove extravesicular dye using 200 mM $NaNO_3$ solution as eluent. The collected vesicles suspension was diluted to 4 mL. Final conditions: ~ 5 mM EYPC; inside: 200 mM $NaNO_3$, 1 mM lucigenin, pH = 7.0; outside: 200 mM $NaNO_3$, pH = 7.0.

Ion transport activity by Lucigenin assay

In clean and dry fluorescence cuvette, 200 mM $NaNO_3$ (1975 µL) and EYPC-LUVs⊃lucigenin (25 µL) were taken. This suspension was placed in a slowly stirring condition in a fluorescence instrument equipped with a magnetic stirrer (at t = 0 s). The fluorescence intensity of lucigenin was monitored at λ_{em} = 535 nm (λ_{ex} = 455 nm) as a course of time. The chloride gradient was created by the addition of 2.0 M NaCl (33.3 µL) at t = 20 s between intra- and extravesicular system, followed by addition of the transporter at t = 100 s. Finally, vesicles were lysed by adding 10% Triton X-100 (25 µL) at t = 300 s for the complete destruction of the chloride gradient. The time scale was normalized using Equation S1.

The time-dependent data were normalized to percent change in fluorescence intensity using Equation S4:

$$I_F = [(I_t - I_0) / (I_\infty - I_0)] \times (-100) \qquad \text{Equation S4}$$

where, I_0 is the initial intensity, I_t is the intensity at time t, and I_∞ is the final intensity after addition of Triton X-100.

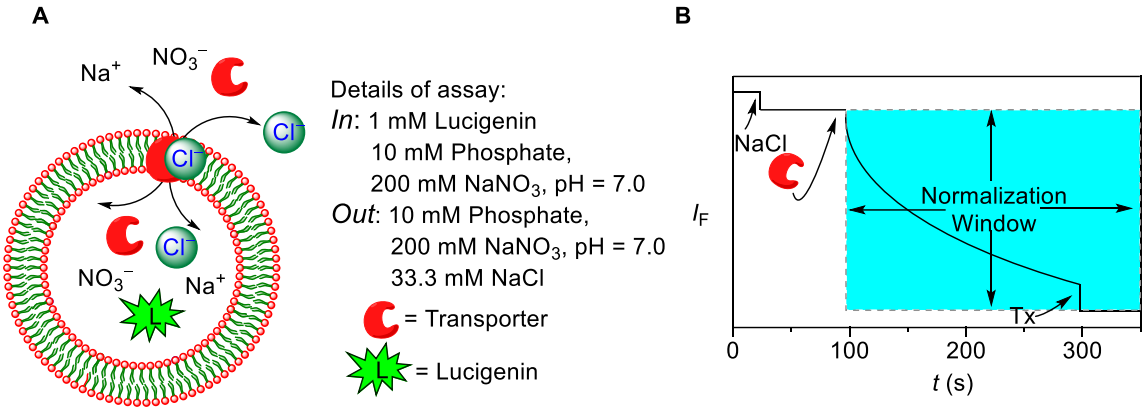

Figure S22. Representation of fluorescence-based ion transport activity assay using EYPC-LUVs⊃Lucigenin (A), and illustration of ion transport kinetics showing normalization window (B).

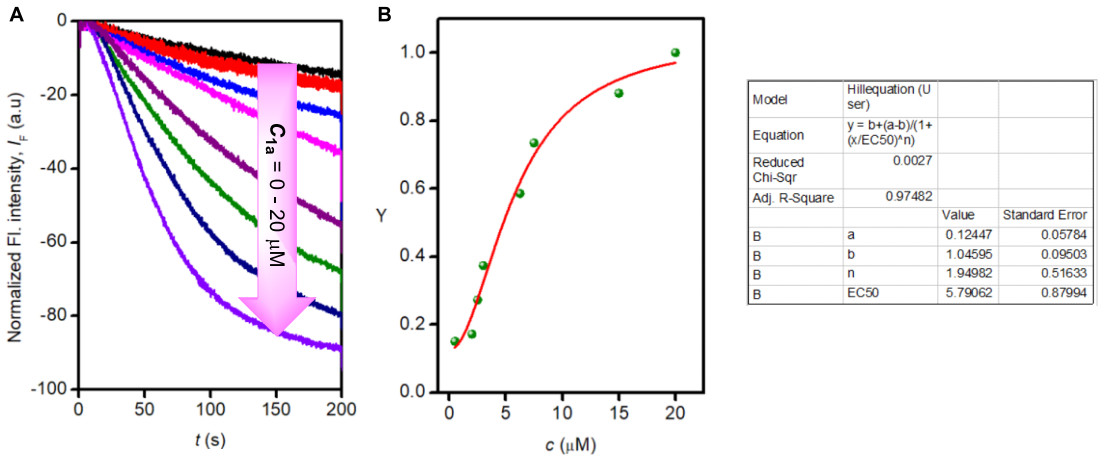

Model	Hillequation (User)		
Equation	y = b+(a-b)/(1+(x/EC50)^n)		
Reduced Chi-Sqr	0.0027		
Adj. R-Square	0.97482		
		Value	Standard Error
B	a	0.12447	0.05784
B	b	1.04595	0.09503
B	n	1.94982	0.51633
B	EC50	5.79062	0.87994

Figure S23. Concentration-dependent activity of **1a** across EYPC-LUVs⊃lucigenin (A), and Hill plot of compound **1a** at t = 180 s to get EC_{50} and n (B).

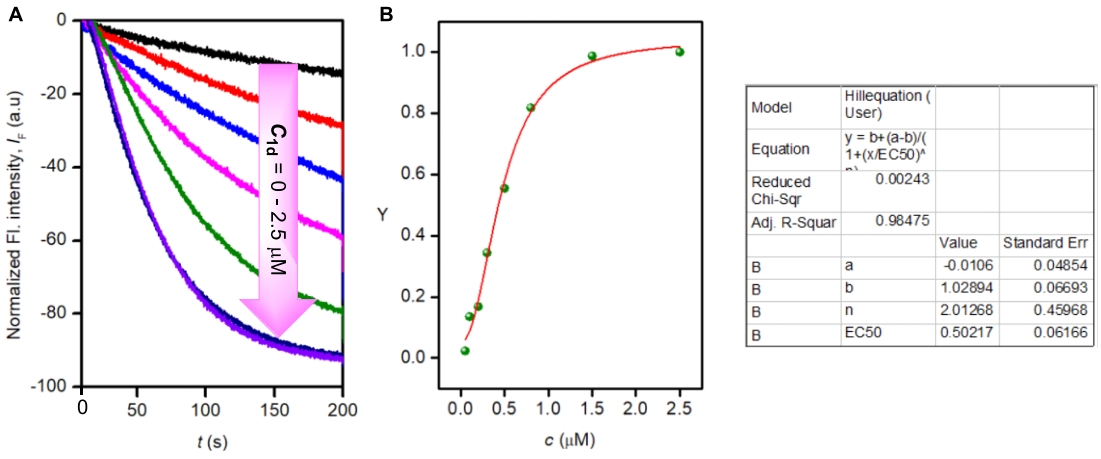

Model	Hillequation (User)		
Equation	y = b+(a-b)/(1+(x/EC50)^		
Reduced Chi-Sqr	0.00243		
Adj. R-Squar	0.98475		
		Value	Standard Err
B	a	-0.0106	0.04854
B	b	1.02894	0.06693
B	n	2.01268	0.45968
B	EC50	0.50217	0.06166

Figure S24. Concentration-dependent activity of **1d** across EYPC-LUVs⊃lucigenin (A), and Hill plot of compound **1d** at t = 180 s to get EC_{50} and n (B).

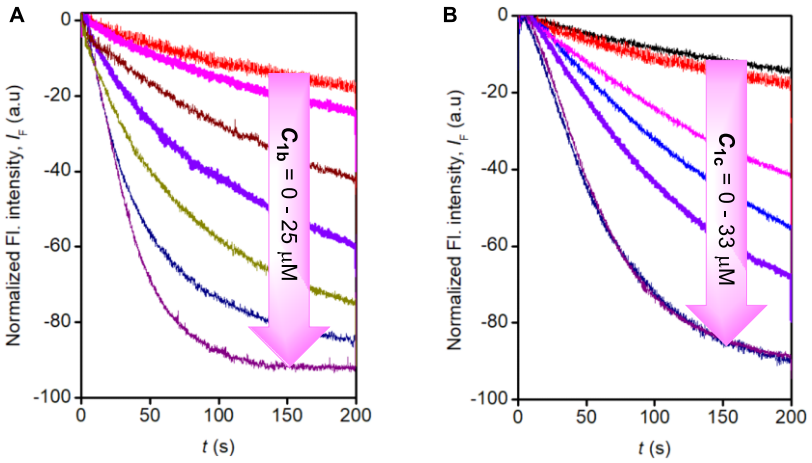

Figure S25. Dose responsive studies of **1b** (A) and **1c** (B) across EYPC- LUVs⊃lucigenin.

C. Ion selective studies

Anion selectivity studies

Preparation of EYPC-LUVs⊃HPTS for anion selectivity: EYPC-LUVs⊃HPTS (~ 5.0 mM EYPC, inside: 1 mM HPTS, 10 mM HEPES, 100 mM NaCl, pH = 7.0 and outside: 10 mM HEPES, 100 mM NaX, pH = 7.0; where, X^- = Cl^-, Br^-, ClO_4^-, NO_3^-, and I^-) were prepared following reported protocol.[S5]

Anion selectivity assay: In clean and dry fluorescence cuvette, 1975 μL HEPES buffer (10 mM HEPES, 100 mM NaX, pH = 7.0; where X = Cl^-, Br^-, I^-, ClO_4^-, and NO_3^-) was taken, followed by addition of 25 μL EYPC-LUVs⊃HPTS. The resulting solution was slowly stirred in a fluorescence instrument equipped with the magnetic stirrer (t = 0 s). The fluorescence intensity of HPTS was observed at λ_{em} = 510 nm (λ_{ex} = 450 nm) as a course of time t, with creating pH gradient by the addition of 20 μL 0.5 M NaOH at t = 20 s, followed by the addition of transporter **1a** (as a DMSO solution) at t = 100 s to initiate ion transport. Finally, vesicles were lysed for the complete destruction of pH gradient by addition of 10% Triton X-100 (25 μL) at t = 300 s. The time axis was normalized according to Equation S1. The time-dependent data were normalized to percent change in intensity using Equation S2.

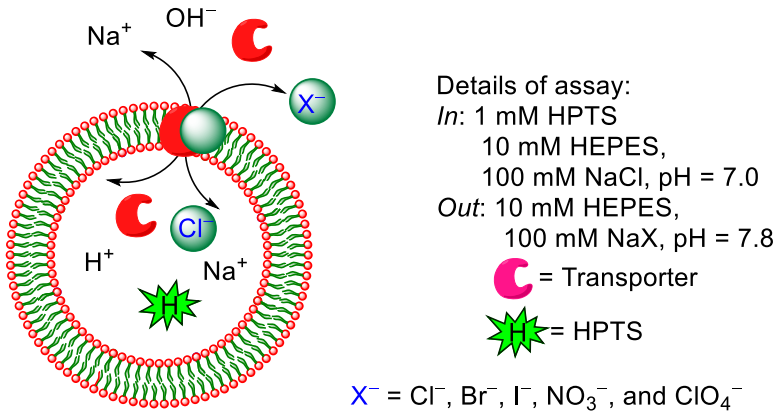

Figure S26. Schematic representation of fluorescence-based anion assay by changing extravesicular anions.

Cation selectivity assay across EYPC-LUVs⊃lucigenin vesicles

The vesicles were prepared by following the same protocol as stated above. In clean and dry fluorescence cuvette, 200 mM $NaNO_3$ (1975 μL) and EYPC-LUVs⊃lucigenin (25 μL) were taken. The suspension was kept in slowly stirring condition in a fluorescence instrument equipped with a magnetic stirrer at t = 0 s. The quenching of fluorescence intensity of lucigenin was monitored as a course of time at λ_{em} = 535 nm (λ_{ex} = 455 nm). At t = 20 s, the chloride gradient was created by addition of 2 M chloride salts (33.3 μL) of different cations MCl (M = Li^+, Na^+, K^+, Rb^+, and Cs^+), followed by addition of transporter **1a** at t = 100 s.

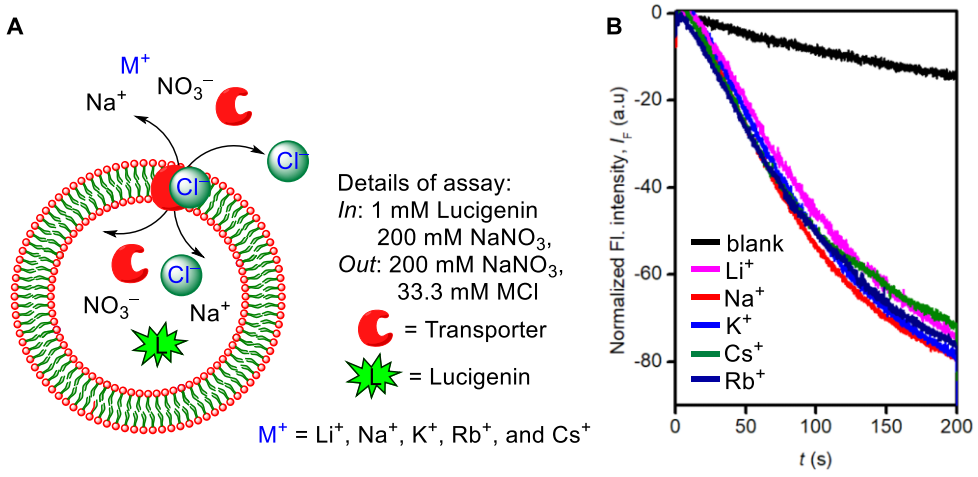

Figure S27. Schematic representation of fluorescence-based cation selectivity assay (A) Cation selectivity of **1a** (1.25 μM) measured by varying external cations (M^+ = Li^+, Na^+, K^+, Rb^+, and Cs^+) across EYPC-LUVs⊃Lucigenin (B).

Finally, vesicles were lysed by the addition of 10% Triton X-100 (25 μL) at t = 300 s to destruct the applied chloride gradient completely. The time scale was normalized using Equation S1 and the time-dependent data were normalized to percent change in fluorescence intensity using Equation S4 respectively.

D. Proof of antiport mechanism by lucigenin assay in the presence of external SO_4^{2-} and NO_3^- anions

Preparation of EYPC-LUVs⊃lucigenin vesicles: In a 10 mL clean and dry round bottom flask, the thin transparent film of egg yolk phosphatidylcholine (EYPC) was formed by drying 1.0 mL egg yolk phosphatidylcholine (EYPC, 25 mg/mL in $CHCl_3$) with providing continuous rotation and purging nitrogen. The transparent thin film was kept under a high vacuum for 4 hours to remove all traces of $CHCl_3$. Then the transparent thin film was hydrated with 1.0 mL aqueous NaCl (200 mM, 1.0 mM Lucigenin) with occasional vortexing at 10 min intervals for 1 h. The resulting suspension was subjected to freeze and thaw cycles (≥ 15, liquid nitrogen, 55 °C water bath) and 21 times extrusion through 200 nm pore size polycarbonate membrane. The size exclusion chromatography (using Sephadex G-50) was performed to remove extravesicular dye using 200 mM NaCl solution as eluent. The collected vesicles suspension was diluted to 4 mL. Final conditions: ~ 5 mM EYPC; inside: 200 mM NaCl, 1 mM lucigenin, pH 7.0; outside: either 200 mM $NaNO_3$ or 200 mM Na_2SO_4.

Ion transport assay

In a clean and dry fluorescence cuvette, either 200 mM of $NaNO_3$ or 200 mM of Na_2SO_4 (1975 μL) and EYPC-LUVs⊃lucigenin (25 μL) were taken. This suspension was placed in a slowly stirring condition in a fluorescence instrument equipped with a magnetic stirrer (at t = 0 s). The fluorescence intensity of lucigenin was monitored at λ_{em} = 535 nm (λ_{ex} = 455 nm) as a course of time. The transporter molecule **1a** was added at t = 100 s. Finally, vesicles were lysed by adding 10% Triton X-100 (25 μL) at t = 300 s for the complete destruction of chloride gradient. NO_3^- transport occurred with the concomitant efflux of Cl^- ions, and on the other hand, SO_4^{2-} being more hydrophilic is not transported easily, suggesting the operation of antiport mechanism (Figure S28).

The time axis was normalized using Equation S1, and the time-dependent data were normalized to percent change in fluorescence intensity using Equation S2.

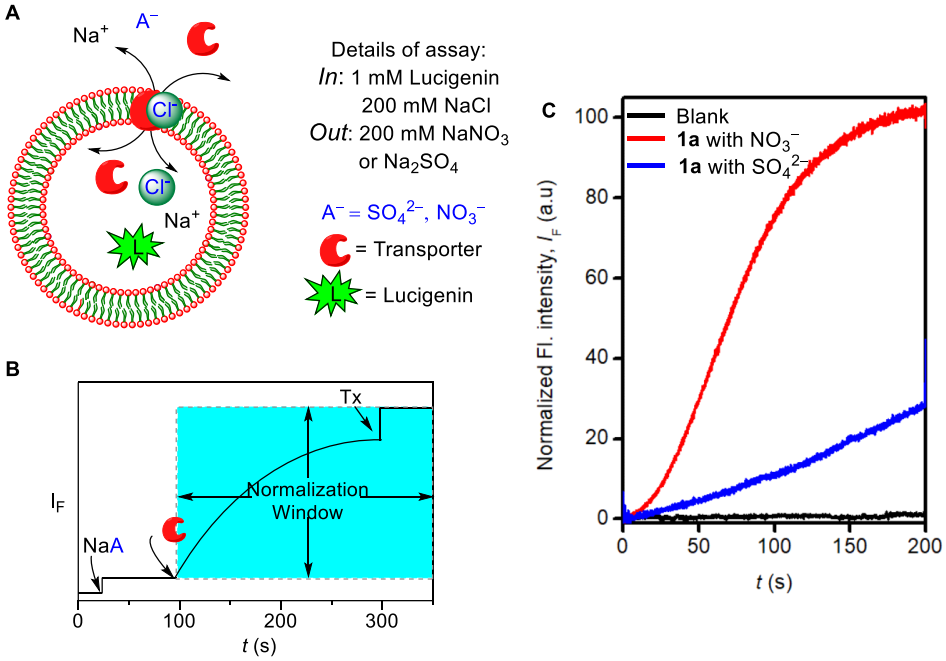

Figure S28. Representation of fluorescence-based antiport assay using EYPC-LUVs⊃lucigenin (A) Representation of ion transport kinetics showing normalization window (B) Efflux of Cl^- ion by **1a** (10 μM) in the presence of either extravesicular SO_4^{2-} or extravesicular NO_3^- ion with isoosmolar intravesicular Cl^- (C).

E. Ion transport studies through chloride-based ion selective electrode

Preparation of ISE vesicles: A chloroform solution (1 mL) of 1-palmitoyl-2-oleoylphosphatidylcholine (EYPC) (25 mg) was evaporated under reduced pressure to give a thin film. The lipid film was dried under a high vacuum for 4 hours. The thin film was rehydrated by vortexing with a potassium chloride solution (300 mM KCl, 5 mM phosphate buffer at pH = 7.2). The lipid suspension was then subjected to fifteen freeze-thaw cycles and was allowed to age for 1 h at room temperature. The suspension was extruded twenty-three times through a 200 nm polycarbonate membrane using an extruder (Avanti, The Mini-Extruder set) to obtain unilamellar vesicles containing KCl (300 mM in 5 mM phosphate buffer at pH = 7.2). Non-encapsulated KCl salts were removed by dialyzing the vesicles three times in a potassium gluconate solution (300 mM, 5 mM phosphate buffer at pH = 7.2).

Ion transport activity in the presence of Valinomycin and Monensin

In a clean and dry glass vial, 50 μL of above lipid solution and 1950 μL of 300 mM K-gluconate of respective pH buffer solutions was taken and kept in slowly stirring condition by a magnetic stirrer (at t = 0 s) and chloride efflux was monitored with time. Transporter

molecule **1a** as DMSO solution was added at t = 50 s, Monensin and Valinomycin as DMSO solutions were added at t = 10 s and finally at t = 300 s, 25 µL of 10% Triton X-100 was added to lyse those vesicles for 100% chloride influx. The chloride efflux for **1a** was monitored in the presence and absence of Monensin and Valinomycin. The value at 50 seconds was set at 0% chloride efflux and the final chloride reading at 300 s was set as 100% chloride efflux. The time axis was normalized using the Equation S5.

$$t = t - 50 \qquad \text{Equation S5}$$

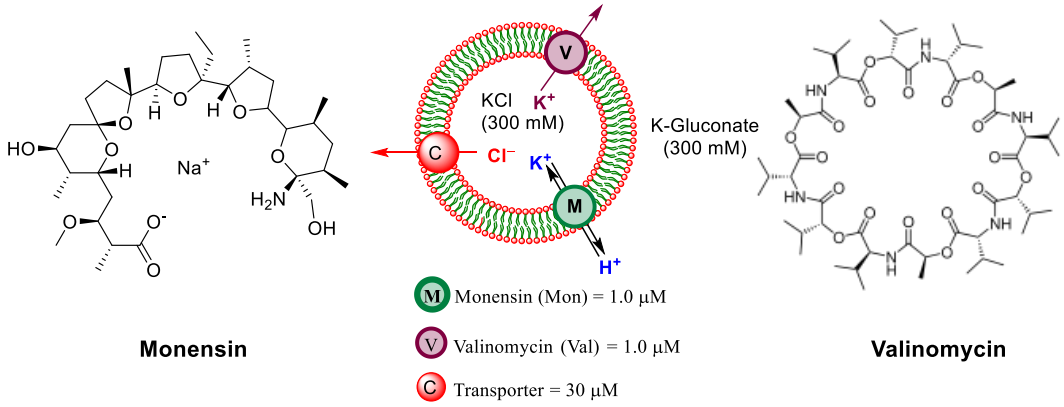

Figure S29. Schematic representation of ISE-based Valinomycin and Monensin assay.

F. U-tube experiments for checking Cl^- transport

This experiment was performed to check whether the chloride ion is transported via a mobile carrier mechanism by a transporter molecule or not. For that, an experiment was set up using a U-tube, where the left arm (Source arm) of the tube was filled with 7.5 mL of 500 mM NaCl solution buffered to pH 7.0 using 5 mM phosphate buffer, and the right arm (receiver arm) of the tube was filled with 7.5 mL of 500 mM $NaNO_3$ solution buffered to pH 7.0 using 5 mM phosphate buffer. Two different salts solutions in two different arms were separated by 15 mL solution of compound **1a** in $CHCl_3$ (1 mM compound 1a, and 1 mM tetrabutylammonium hexafluorophosphate) in such a way that two salts solutions never come contact with each other. Here transport of chloride ions is only possible via mobile carrier mechanism due to the long length of the $CHCl_3$ layer, which does not allow any ion channel formation. For checking transport activity via carrier mechanism, chloride ion concentration in the receiver arm was measured by chloride ion selective electrode. The gradual increase of chloride ion concentration (Figure S30) was measured in a fixed time interval for the time period of 10 days, gave evidence in support of the mobile carrier mechanism. In a control

experiment, no increase in chloride ion concentration was observed when compound **1a** was not added in the $CHCl_3$ layer.

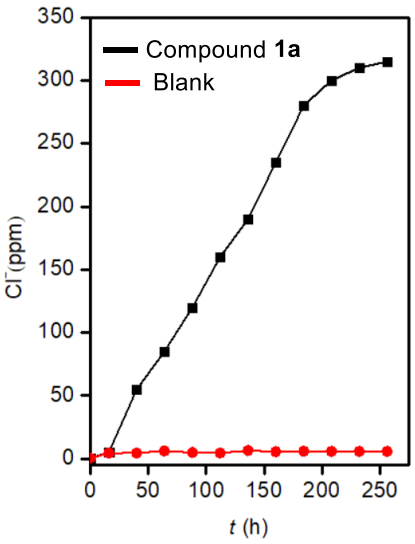

Figure S30. Change of chloride ion concentration in a U-tube experiment with and without compound **1a** (1.0 mM).

VII. Photoisomerization Studies by UV-Vis and ^{1}H NMR

A. UV-Vis studies

Photoisomerizations of compounds **1a**, **1b**, **1c** and **1d** were carried out in CH_3CN. Initially, stock solutions of these compounds (2 mM in CH_3CN) were prepared in different vials, and covered with an aluminium foil.

In a 2 mL UV cuvette, was placed either 1900 µL of CH_3CN and 100 µL of either **1a**, **1b**, **1c** or **1d** (2 mM in CH_3CN) was added to get the final concentration of 100 µM.

The cuvette was placed in a UV-Vis spectrometer and the UV-Vis spectrum was recorded.

***trans* to *cis* Isomerization:** Subsequently, each of these samples was irradiated at λ = 312 nm using UV tubes (8 × 3 Watt) for varied time intervals to isomerize the acylhydrazone moiety. After each irradiation, the UV-Vis spectrum was recorded (Figures S31A, S32A, S33A, and S34A).

^{1}H NMR studies: *trans* (*E*) to *cis* (*Z*) photoisomerization: For monitoring the *trans* (*E*) to *cis* (*Z*) isomerization by ^{1}H NMR, a sample of **1a**, **1b**, **1c**, or **1d** (4.0×10^{-3} M) in CD_3CN was prepared in an NMR tube and then irradiated at λ = 312 nm using UV tubes (8 × 3 Watt) for

30 min and then the ^{1}H NMR data before and after photoirradiation were compared. The *trans* to *cis* ratio after photoirradiation for **1a**, **1b**, **1c**, and **1d** were 15:85, 10:90, 17:83, and 62:38, respectively (Figures S31B, S32B, S33B and S34B).

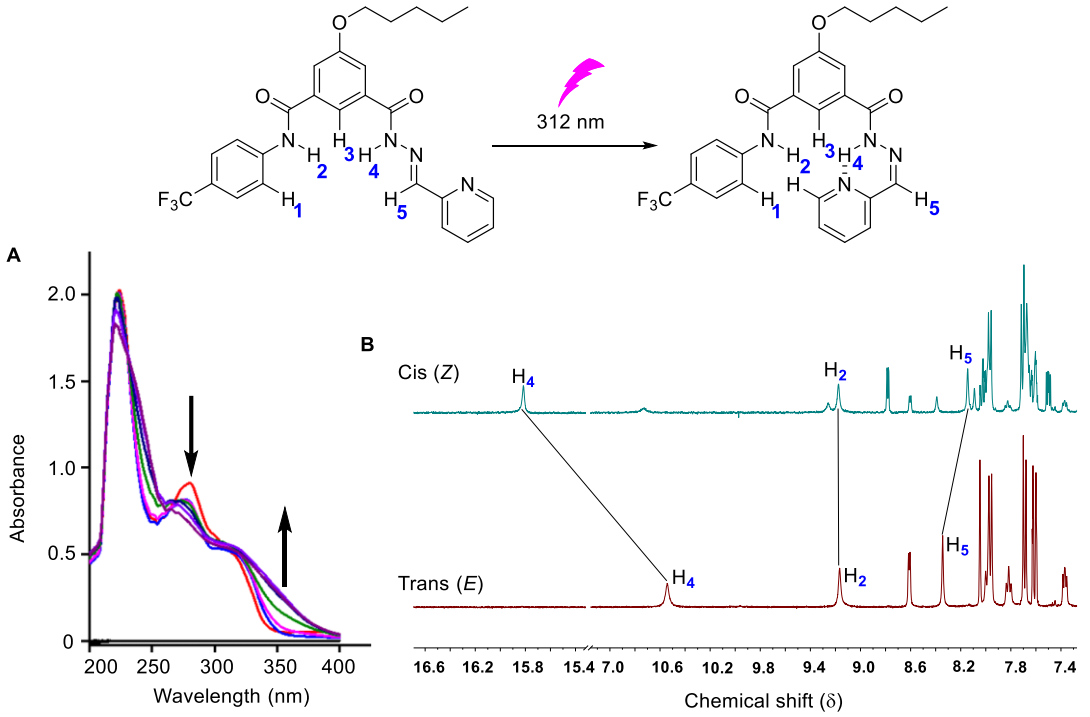

Figure S31. UV-Vis spectral changes for **1a** (100 μM) upon irradiation with 312 nm using UV tubes (8 × 3 Watt) (t = 0–10 min) (A). Partial 400 MHz ^{1}H NMR spectrum of **1a** (4.0×10^{-3} M, down) in CD_3CN at 25 °C, and that of photoirradiated sample of **1a** (top) by 312 nm light for 30 min (B).

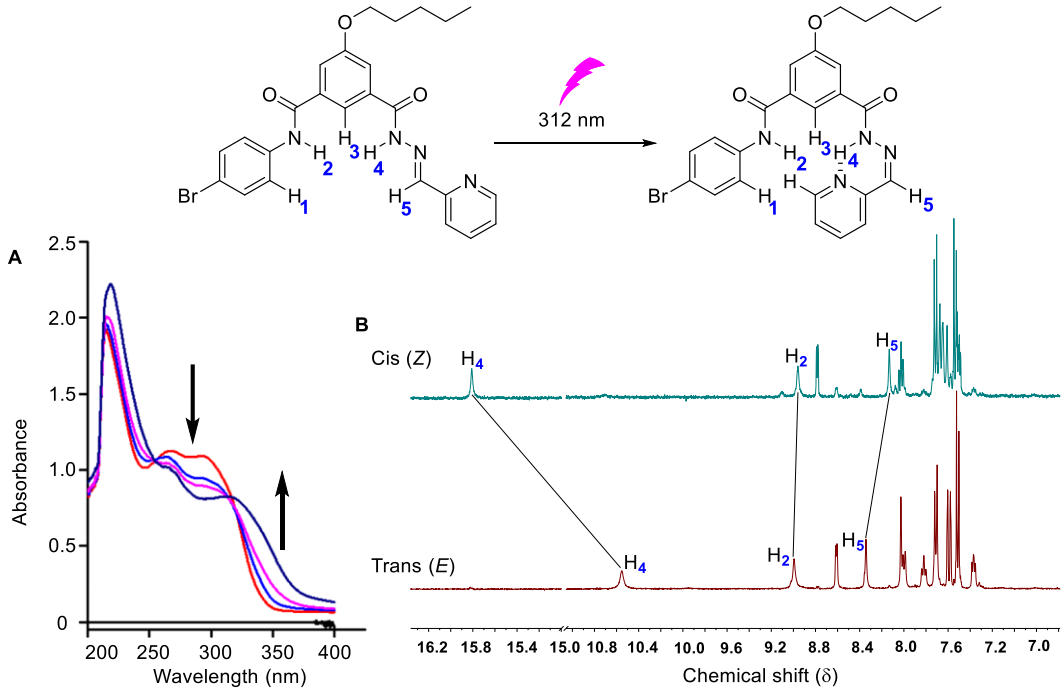

Figure S32. UV-Vis spectral changes for **1b** (100 μM) upon irradiation with 312 nm using UV tubes (8 × 3 Watt) (t = 0–10 min) (A). Partial 400 MHz ^{1}H NMR spectrum of **1b** (4.0 × 10^{-3} M, down) in CD_3CN at 25 °C, and that of photoirradiated sample of **1b** (top) by 312 nm light for 30 min (B).

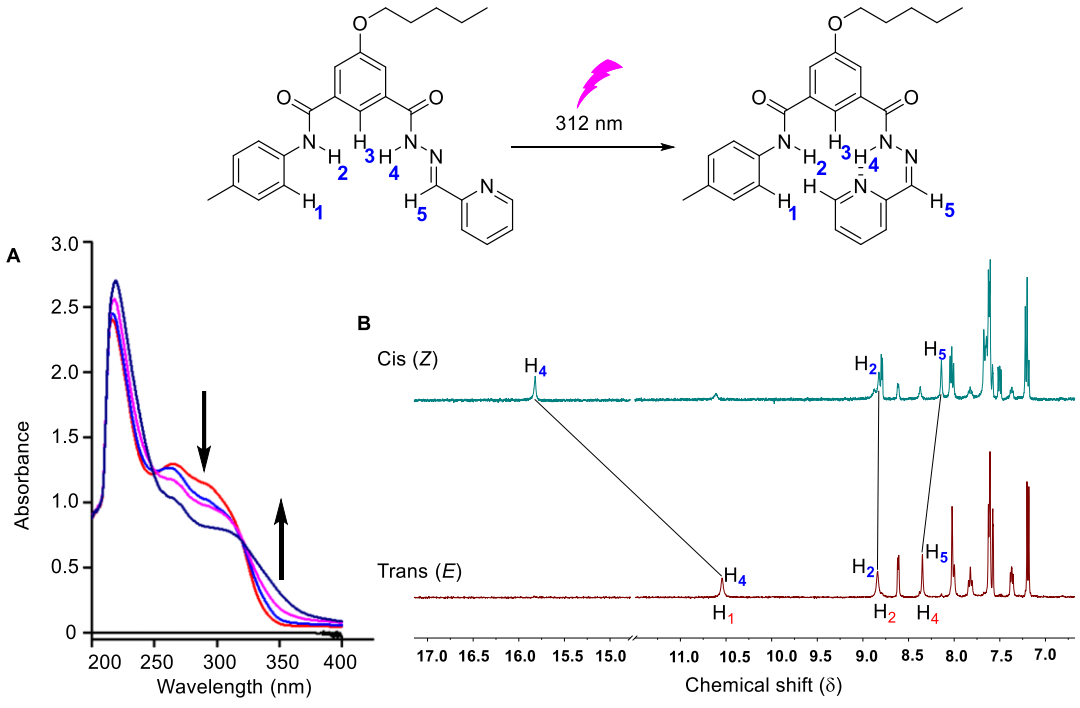

Figure S33. UV-Vis spectral changes for **1c** (100 μM) upon irradiation with 312 nm using UV tubes (8 × 3 Watt) (t = 0-10 min) (A). Partial 400 MHz ^{1}H NMR spectrum of **1c** (4.0 × 10^{-3} M, down) in CD_3CN at 25 °C, and that of photoirradiated sample of **1c** (top) by 312 nm light for 30 min (B).

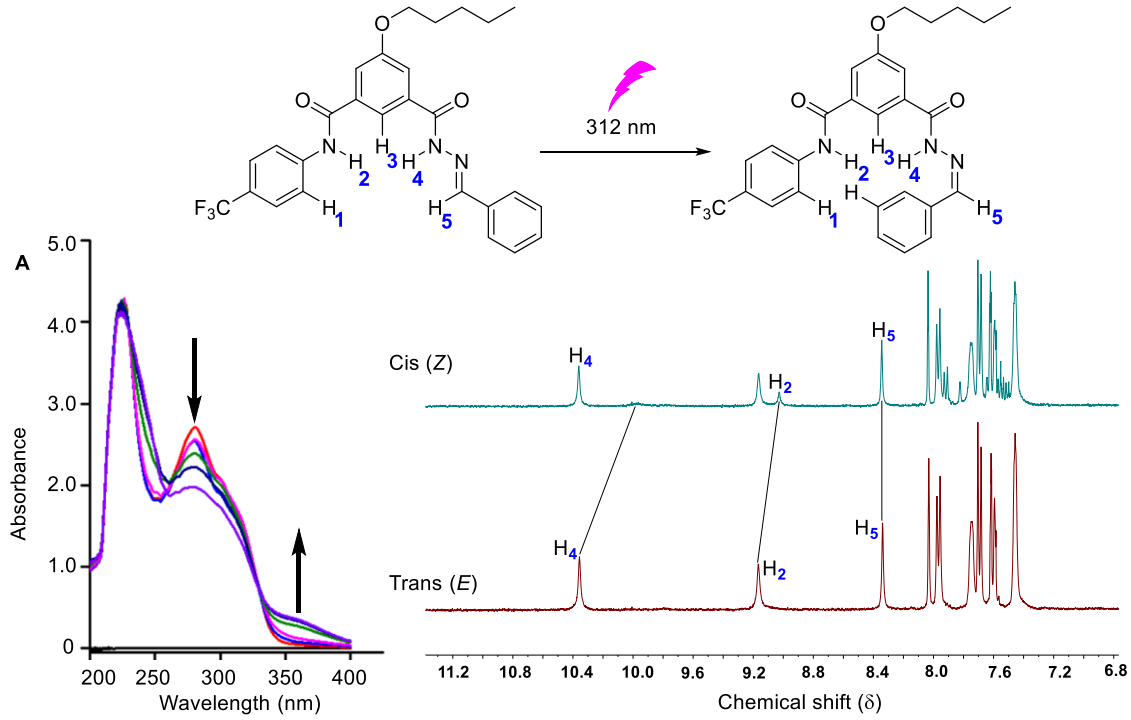

Figure S34. UV-Vis spectral changes for **1d** (100 μM) upon irradiation with 312 nm of light using UV tubes (8 × 3 Watt) (t = 0-10 min) (A). Partial 400 MHz ^{1}H NMR spectrum of **1d** (4.0×10^{-3} M, down) in CD_3CN at 25 °C, and that of photoirradiated sample of **1d** (top) by 312 nm light for 30 min (B).

Thermal stability: To study the stability of **1a** and **1d** in photoisomerized *Z* state, **1a-*E*** and **1d-*E*** in CD_3CN were irradiated at 312 nm to photoisomerize them into **1a-*Z*** and **1d-*Z*** form. After that, the photoisomerized samples were kept in the dark and ^{1}H NMR was recorded at different intervals of time. No significant change was observed for **1a-*Z*** during 30 days while keeping in dark Figure S35. On the other hand, compound **1d-*E*** was poorly photoisomerized into the **1d-*Z*** state with 62:38 *E*:*Z* at the PSS. In addition to this, the photoisomerized **1d-*Z*** state got thermally relaxed back fully within one day Figure S36. These results are the outcome of the presence of intramolecular hydrogen bonding in the photoisomerized *Z* state of **1a** between the pyridine nitrogen and acylhydrazone N–H_3, which shall stabilize it. The lack of this intramolecular hydrogen bonding in **1d** leads to its poor photoisomerization and low thermal stability.

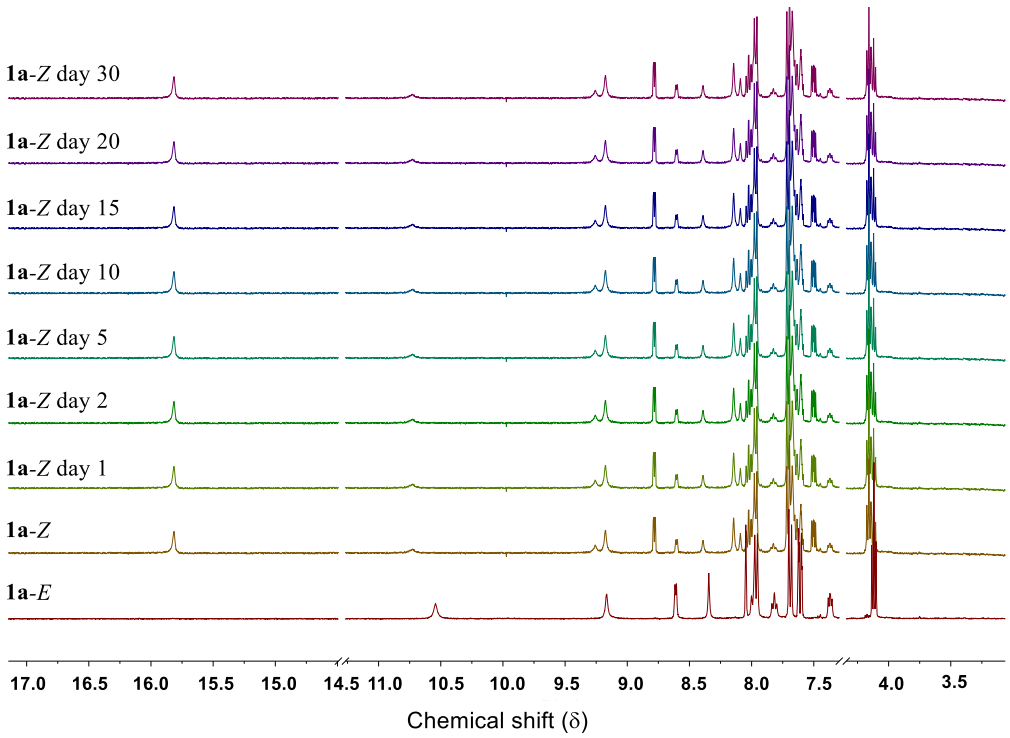

Figure S35. Overlapped ^{1}H NMR spectra of **1a-*Z*** in acetonitrile-d_3 after 1 and 30 days of standing in the dark. No significant changes were observed in the spectra within the investigated time.

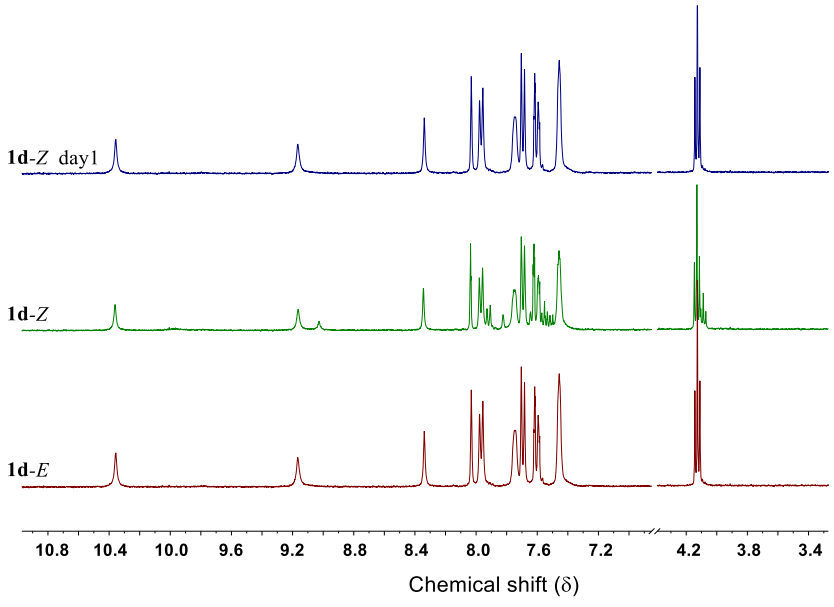

Figure S36. Overlapped ^{1}H NMR spectra of **1d-*Z*** in acetonitrile-d_3 after day of standing in the dark. **1d**–***E*** form was regained back within 1d of thermal relaxation.

Acid-catalyzed reversible photoisomerization studies: Initially, ^{1}H NMR was recorded for **1a**–*E* in acetonitrile-d_3.The sample was then irradiated with 312 nm of light using UV tubes

(8 × 3 Watt) for 35 min to convert **1a**–***E*** to **1a**–***Z***. The **1a**–***Z*** sample was then first treated with 5 equiv. of TFA followed by the addition of 5 equiv. of TEA to generate the initial **1a**–***E*** form (Figure S37). This process of photoirradiation and acid/base reactivation process was repeated for a number of cycles without the loss of efficiency (Figure 5B in manuscript).

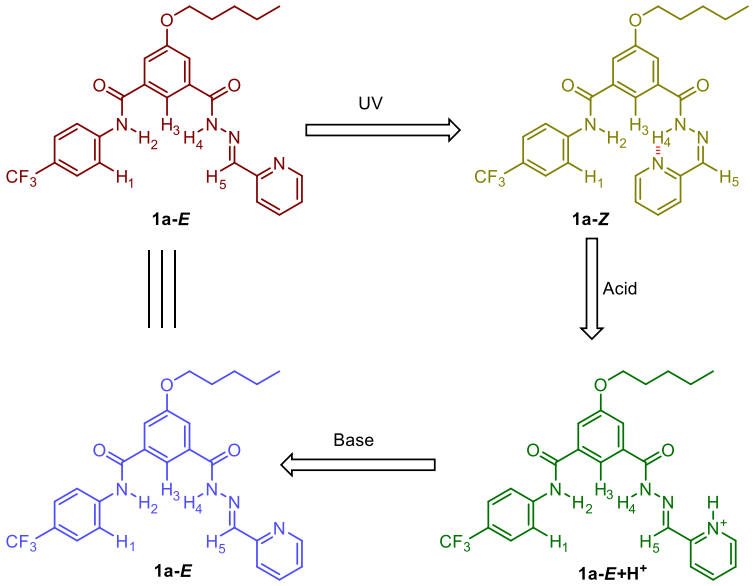

Scheme S2. Proposed photo and acid-induced switching cycle of the receptor **1a** between the binding *E* and non-binding *Z* isomers.

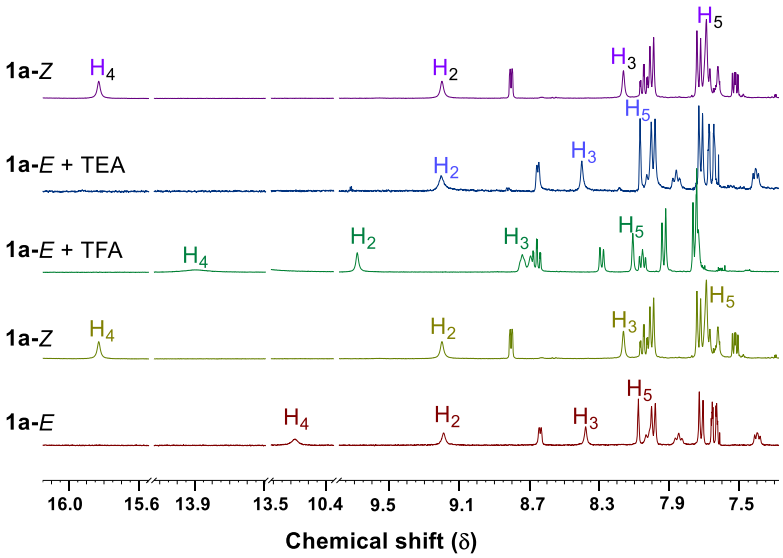

Figure S37. ^{1}H NMR (acetonitrile-d_3) spectra of one photo/acid switching cycle (bottom to top) in the *E*/*Z* isomerization of **1a**-***E*** (2 mM). One cycle involves 3 steps: 1) photoisomerization of **1a**-***E*** to **1a**-***Z*** (312 nm, 30 min, 90% PSS); 2) acid-induced quantitative back-isomerization to protonated **1a**-***E***; 3) neutralization of the protonated **1a**-***Z*** with TEA restoring the non-protonated **1a**-***E***.

VIII. Stimuli-Responsive Ion Transport Activity

Photodeactivation of ion transport through EYPC-LUVs⊃HPTS assay

The EYPC-LUVs⊃HPTS vesicles were prepared using the same protocol as stated above. In a clean and dry fluorescence cuvette, 100 mM NaCl (1975 µL) and EYPC-LUVs⊃HPTS (25 µL) were taken. This suspension was placed in a slowly stirring condition in a fluorescence instrument equipped with a magnetic stirrer. The fluorescence intensity of lucigenin was monitored at λ_{em} = 510 nm (λ_{ex} = 450 nm) as a course of time. The pH gradient was created by the addition of 2.0 M NaOH (25 µL) at *t* = 20 s between intra- and extravesicular system, followed by the addition of transporter **1a** at *t* = 100 s. Finally, vesicles were lysed by addition of 10% Triton X-100 (25 µL) at *t* = 300 s for the complete destruction of the pH gradient. Initially, the transport activity of the compound **1a** (0.3 µM, using a stock solution of 1 mM in acetonitrile was recorded. Subsequently, the stock sample was irradiated at λ = 312 nm using UV tubes (8 × 3 Watt) for 0 to 30 min to photoisomerize the acylhydrazone subunit, and the transport activity using each photoisomerized sample was recorded at different time intervals. Photoisomerization leads to a substantial decrease in transport activity (Figure S38A).

Furthermore, the transport activity of **1a** was monitored by keeping the sample in the dark in the *cis* photoisomerized form. There was no significant increment in the transport activity during this time of 9 h (Figure S38B), which showed its better thermal stability.

The time axis was normalized using Equation S1, and the time-dependent data were normalized to percent change in fluorescence intensity using Equation S2.

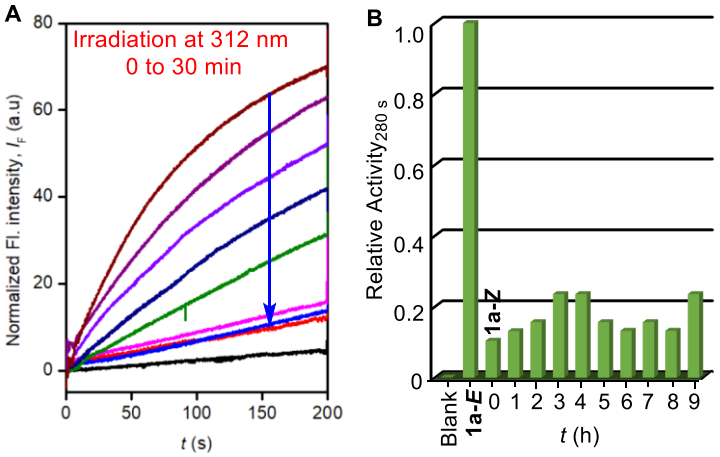

Figure S38. Transport activity of **1a** after irradiation at 312 nm for 0-30 min (A) Ion transport of photoisomerized **1a** while keeping the sample in the dark for 0-9 h (B**)**

Stimuli-responsive reversible ion transport activity through ISE studies

Preparation of ISE vesicles: A chloroform solution (1 mL) of 1-palmitoyl-2-oleoylphosphatidylcholine (EYPC) (25 mg) was evaporated under reduced pressure to give a thin film. The lipid film was dried under a high vacuum for 4 hours. The thin film was rehydrated by vortexing with a sodium chloride solution (500 mM NaCl, 10 mM phosphate buffer at pH = 7.0). The lipid suspension was then subjected to fifteen freeze–thaw cycles and was allowed to age for 1 h at room temperature. The suspension was extruded twenty-three times through a 200 nm polycarbonate membrane using an extruder (Avanti, The Mini-Extruder set) to obtain unilamellar vesicles containing NaCl (500 mM in 10 mM phosphate buffer at pH = 7). Non-encapsulated NaCl salts were removed by dialyzing the vesicles three times in a sodium nitrate solution (500 mM, 10 mM phosphate buffer at pH = 7.0).

Switchable ion transport studies using ion selective electrode

In a clean and dry glass vial, 50 μL of above lipid solution and 1950 μL of 500 mM $NaNO_3$ of respective pH buffer solutions were taken and kept in slowly stirring condition by a magnetic stirrer (at t = 0 s) and chloride efflux was monitored with time. Transporter molecule **1a** as acetonitrile solution was added at t = 50 s, at t = 250 s, 25 μL of 10% Triton X-100 was added to lyse the vesicles for 100% chloride influx. Initially, the chloride efflux was recorded for **1a** (30 μM) using the stock solution of 5 mM of **1a**. Subsequently, the stock solution was photoirridiated for 30 min using 312 nm UV tubes and ion transport activity was recorded. The ion transport activity of **1a** was greatly reduced upon photoirradiation at 312 nm, likely due to the photoisomerization of **1a-*E*** form to **1a-*Z*** form. Eventually, to this photoisomerized stock solution was added triflic acid (5 equiv.) and the solution was kept for 30 min to get the **1a-*E*** form back. After 30 min, triethylamine (TEA, 5 equiv.) was added to neutralize the solution and the chloride efflux was recorded again. The activity was significantly regained back upon the treatment of acid and base (Figure S39C). This process of alternative photoirradiation and acid/base reactivation process was repeated for three cycles (Figure 5B in the manuscript). Finally, the value at 50 seconds was set at 0% chloride efflux and the final chloride reading at 250 s was set as 100% chloride efflux. The time axis was normalized using the Equation 5.

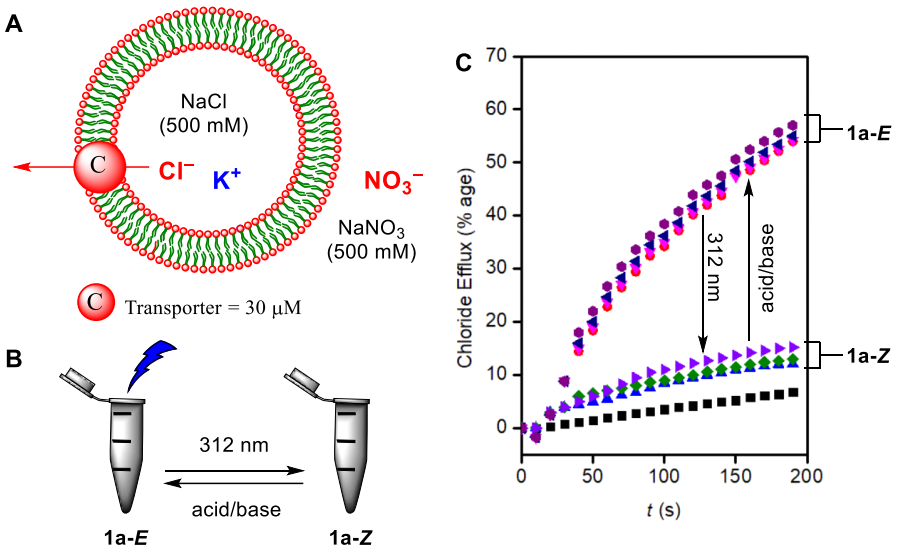

Figure S39. Schematic representation of ISE vesicles (A). **1a-*E*** to **1a-*Z*** Photoisomerization and acid/base reactivation process of **1a** acetonitrile solution (5 mM). Chloride efflux of **1a** in *E* and *Z* forms (C).

IX. X-Ray Crystallographic Studies

General procedure for crystallization

The solution of **1d** (10 mg) in acetonitrile was heated with TBACl salt (05 equiv.) in a 5 mL of glass vial and then filtered to separate any undissolved component. The solution was then left in a stable place to evaporate slowly. After few days, colorless needle-like crystalline material precipitated from the vial. Suitable crystals were chosen for the X-ray measurement.

X-ray single crystal diffraction analysis

The single-crystal X-ray diffraction (SCXRD) analysis of compound **1d** was performed on a Bruker Smart Apex Duo diffractometer using Mo Kα radiation (λ = 0.71073Å). The crystal structures were solved using intrinsic methods and then refined by full-matrix least-squares against F^2 using all data by using SHELXL-2014/7 built in the Apex-3 package.[S6] The crystallographic refinement data for compound **1d** are listed in **(Table S2)**. All the non-hydrogen atoms were refined anisotropically if not stated otherwise. Hydrogen atoms were constructed in geometric positions to their parent atoms.[S7] Some of the atom positions (CF_3 group) disordered sites and their occupancies were modeled using the different crystallographic constrain commands. The DIAMOND-3.1 software was used to describe the

bond length, bond angles and various structural illustrations of compound **1d** with chloride ion.

Table S2. Crystallographic data for compound **1d–Cl⁻** at 100 K.

Crystallographic details	**Compound 1d–Cl⁻**
Chemical formula	$C_{43}H_{62}ClF_3N_4O_4$
Formula weight (g/mol)	791.41
Temperature	100(2)K
Crystal system	Monoclinic
Space group	*P* 2/*n*
a (Å); α (°)	20.366(9); 90
b (Å); β (°)	8.237(4); 110.575(9)
c (Å); γ (°)	27.647(12); 90
V (Å^3); Z	4342.(3); 4
ρ (calc.) g cm^{-3}	1.211
μ(Mo K$_\alpha$) mm^{-1}	0.145
2θ$_{max}$ (°)	46.5
R(int)	0.2887
Completeness to θ	99.4
Data / param.	6200/494
GOF	1.028
R1 [F>4σ(F)]	0.0987
wR2 (all data)	0.2971
max. peak/hole (e.Å^{-3})	0.995/-0.628

Table S3. Crystallographic data for compound **1d–Cl⁻** at 100 K.

D-H…A	**d(D-H)**	**d(H…A)**	**d(D-A)**	**<DHA**	**Symmetry operations**
N(1)-H(1)…Cl(1)	0.8800(4)	2.4576(11)	3.3062(15)	162.127 (75)	x, y, z
N(3)-H(3)…Cl(1)	0.8800(3)	2.4620(9)	3.3151(11)	163.470(45)	x, y, z
C(1)-H(1A)…Cl(1)	0.9500(4)	2.8173(9)	3.6590(13)	148.196(56)	x, y, z
C(12P)-H(12P)…Cl(1)	0.9500(3)	2.5028(7)	3.4454(10)	171.587(50)	x, y, z
C(17P)-H(17P)…Cl(1)	0.9500(4)	2.8074(10)	3.7202(14)	161.406(45)	x, y, z
C(18P)-H(18P)…Cl(1)	0.9500(3)	2.7404(10)	3.5484(12)	143.379(49)	x, y, z

Table S4. Selected bond lengths [Å] and angles [°] for compound **1d–Cl⁻** at 100 K.

Bond length	Bond length	Bond angle	Bond angle
N1-N2: 1.384(7)	C3P-C4P: 1.39	N2-N1-C2: 118.3(6)	H13A-C13C-H13B: 108.0
N1-H1: 0.88	C4P-C5P: 1.39	C2-N1-H1: 120.8	C13C-C14C-H14A: 108.4
N3-C8: 1.381(9)	C5P-H5P: 0.95	C8-N3-C13P: 126.3(5)	C13C-C14C-H14B: 108.4
N3-H3: 0.88	C7P-C8P: 1.39	C13P-N3-H3: 116.8	H14A-C14C-H14B: 107.5
O1-C3: 1.433(12)	C8P-C9P: 1.39	N2-C1-C4P: 121.7(6)	C16C-C15C-H15A: 108.3
O3-C2: 1.183(7)	C9P-C10P: 1.39	C4P-C1-H1A: 119.1	C16C-C15C-H15B: 108.3
C1-H1A: 0.95	C10P-H10P: 0.95	O3-C2-C7P: 123.0(7)	H15A-C15C-H15B: 107.4
C3-C4: 1.525(13)	C12P-H12P: 0.95	O1-C3-C4: 100.6(9)	C15C-C16C-H16A: 109.4
C3-H3B: 0.99	C13P-C18P:1.39	C4-C3-H3A: 111.6	C15C-C16C-H16B: 109.4
C4-H4A: 0.99	C14P-H14P: 0.95	C4-C3-H3B: 111.6	H16A-C16C-H16B: 108.0
C5-C6: 1.513(14)	C15P-H15P: 0.95	C5-C4-C3: 132.7(12)	C18C-C17C-H17A: 108.5
C5-H5B: 0.99	C16P-C9: 1.461(9)	C3-C4-H4A: 104.1	C18C-C17C-H17B: 108.5
C6-H6A: 0.99	C17P-H17P: 0.95	C3-C4-H4B: 104.1	H17A-C17C-H17B: 107.5
C7-H7A: 0.98	N1C-C24C: 1.515(7)	C4-C5-C6: 121.4(12)	C17C-C18C-H18B: 109.5
C7-H7C: 0.98	N1C-C25C: 1.517(7)	C6-C5-H5A: 107.0	C17C-C18C-H18C: 109.5
C1P-C2P: 1.39	C11C-C12C: 1.486(10)	C6-C5-H5B: 107.0	H18B-C18C-H18C: 109.5
C1P-H1P: 0.95	C11C-H11B: 0.98	C7-C6-C5: 106.8(11)	C15C-N2C-C14C: 110.5(3)
C2P-H2P: 0.95	C12C-C13C: 1.515(9)	C5-C6-H6A: 110.4	C15C-N2C-C14C: 111.3(4)
C3P-H3P: 0.95	C12C-H12B: 0.99	C5-C6-H6B: 110.4	C14C-N2C-C14C: 106.7(6)
C5P-C6P: 1.39	C13C-H13A: 0.99	C6-C7-H7A: 109.5	C22C-C21C-H21B: 109.5
C6P-H6P: 0.95	C14C-N2C: 1.520(7)	H7A-C7-H7B: 109.5	C22C-C21C-H21C: 109.5
C7P-C12P: 1.39	C14C-H14B: 0.99	H7A-C7-H7C: 109.5	H21B-C21C-H21C: 109.5
C8P-H8P: 0.95	C15C-N2C: 1.518(7)	O2-C8-N3: 121.9(8)	C21C-C22C-H22A: 109.0
C10P-C11P: 1.39	C15C-H15B: 0.99	N3-C8-C11P: 117.5(6)	C21C-C22C-H22B: 109.0
C11P-C12P: 1.39	C16C-H16A: 0.99	C2P-C1P-H1P: 120.0	H22A-C22C-H22B: 107.8
C13P-C14P: 1.39	C17C-C18C: 1.493(11)	C1P-C2P-C3P: 120.0	C24C-C23C-H23A: 109.5
C14P-C15P: 1.39	C17C-H17B: 0.99	C3P-C2P-H2P: 120.0	C24C-C23C-H23B: 109.5
C15P-C16P: 1.39	C18C-H18B: 0.98	C4P-C3P-H3P: 120.0	H23A-C23C-H23B: 108.1
C16P-C17P: 1.39	N2C-C15C:1.518(7)	C3P-C4P-C5P: 120.0	C23C-C24C-H24A: 108.3
C17P-C18P: 1.39	C21C-C22C: 1.500(9)	C5P-C4P-C1: 118.4(4)	C23C-C24C-H24B: 108.3
C18P-H18P: 0.95	C21C-H21B: 0.98	C6P-C5P-H5P: 120.0	H24A-C24C-H24B: 107.4
N1C-C24C: 1.515(7)	C22C-C23C: 1.505(9)	C5P-C6P-C1P: 120.0	C26C-C25C-H25A: 108.2

N1C-C25C: 1.517(7)	C22C-H22B: 0.99	C1P-C6P-H6P: 120.0	C26C-C25C-H25B: 108.2
C11C-H11A: 0.98	C23C-H23A: 0.99	C8P-C7P-C2: 115.8(4)	H25A-C25C-H25B: 107.4
C11C-H11C: 0.98	C24C-H24A: 0.99	C9P-C8P-C7P: 120.0	C25C-C26C-H26A: 109.8
C12C-H12A: 0.99	C25C-C26C: 1.511(8)	C7P-C8P-H8P: 120.0	C25C-C26C-H26B: 109.8
C13C-C14C: 1.517(8)	C25C-H25B: 0.99	O1-C9P-C8P: 124.9(5)	H26A-C26C-H26B: 108.2
C13C-H13B: 0.99	C26C-H26A: 0.99	C9P-C10P-C11P: 120.0	C26C-C27C-H27A: 109.0
C14C-H14A: 0.99	C27C-C28C: 1.540(9)	C11P-C10P-H10P: 120.0	C26C-C27C-H27B: 109.0
C15C-C16C: 1.510(9)	C27C-H27B: 0.99	C10P-C11P-C8: 116.0(4)	H27A-C27C-H27B: 107.8
C15C-H15A: 0.99	C28C-H28B: 0.98	C11P-C12P-C7P: 120.0	C27C-C28C-H28B: 109.5
C16C-C17C: 1.511(10)	C9-F3': 1.274(16)	C7P-C12P-H12P: 120.0	C27C-C28C-H28C: 109.5
C16C-H16B: 0.99	C9-F1: 1.303(11)	C14P-C13P-N3: 123.2(4)	H28B-C28C-H28C: 109.5
C17C-H17A: 0.99	C9-F3: 1.364(10)	C15P-C14P-C13P: 120.0	F3'-C9-F2': 107.7(13)
C18C-H18A: 0.98	N1-C2: 1.388(8)	C13P-C14P-H14P: 120.0	F1-C9-F3: 107.1(9)
C18C-H18C: 0.98	N2-C1: 1.261(8)	C14P-C15P-H15P: 120.0	F2-C9-C16P: 111.2(8)
N2C-C14C: 1.520(7)	N3-C13P: 1.398(6)	C15P-C16P-C17P: 120.0	F2'-C9-C16P: 122.1(9)
C21C-H21A: 0.98	O1-C9P: 1.371(6)	C17P-C16P-C9: 119.4(5)	F3'-C9-F1': 98.4(12)
C21C-H21C: 0.98	O2-C8: 1.218(9)	C18P-C17P-H17P: 120.0	C16P-C9-F1': 109.3(8)
C22C-H22A: 0.99	C1-C4P: 1.454(7)	C17P-C18P-C13P: 120.0	C27C-C26C-H26B: 109.8
C23C-C24C: 1.504(8)	C2-C7P: 1.476(7)	C13P-C18P-H18P: 120.0	C26C-C27C-C28C: 112.8(6)
C23C-H23B: 0.99	C3-H3A: 0.99	C24C-N1C-C25C: 110.9(3)	C28C-C27C-H27A: 109.0
C24C-H24B: 0.99	C4-C5: 1.252(11)	C24C-N1C-C25C: 110.8(3)	C28C-C27C-H27B: 109.0
C25C-H25A: 0.99	C4-H4B: 0.99	C25C-N1C-C25C: 106.5(6)	C27C-C28C-H28A: 109.5
C26C-C27C: 1.515(9)	C5-H5A: 0.99	C12C-C11C-H11B: 109.5	H28A-C28C-H28B: 109.5
C26C-H26B: 0.99	C6-C7: 1.386 (15)	C12C-C11C-H11C: 109.5	H28A-C28C-H28C: 109.5
C27C-H27A: 0.99	C6-H6B: 0.99	H11B-C11C-H11C: 109.5	F2-C9-F1: 112.4(10)
C28C-H28A: 0.98	C7-H7B: 0.98	C11C-C12C-H12A: 108.7	F2-C9-F3: 104.5(10)
C28C-H28C: 0.98	C8-C11P: 1.480(9)	C11C-C12C-H12B: 108.7	F3'-C9-C16P: 120.1(11)
C9-F2: 1.279(11)	C1P-C6P: 1.39	H12A-C12C-H12B: 107.6	F1-C9-C16P: 112.7(9)
C9-F2': 1.341(16)	C2P-C3P: 1.39	C12C-C13C-H13A: 109.4	F3-C9-C16P: 108.4(7)
C9-F1': 1.490(16)		C12C-C13C-H13B: 109.4	F2'-C9-F1': 92.8(11)

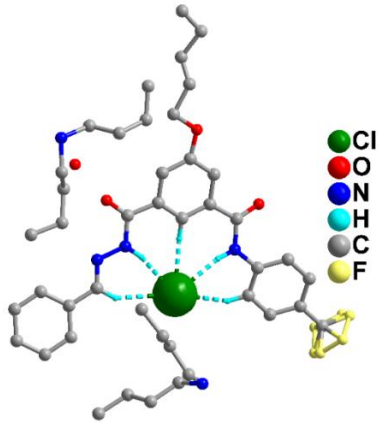

Figure S40. The asymmetric unit of **1d** with TBACl (Here the H-atoms are removed for structure clarity).

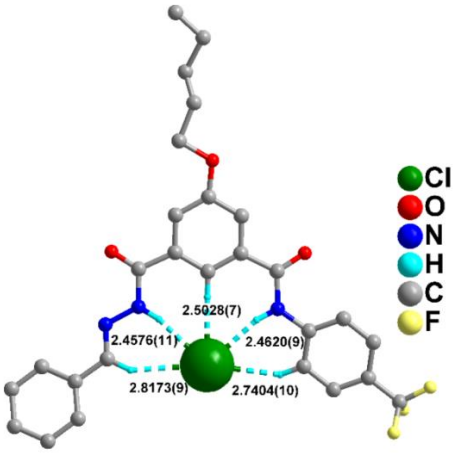

Figure S41. Hydrogen-bonded crystal structure of **1d** with Cl^- in 1:1 receptor:Cl^- binding mode. Some of the aliphatic and aromatic H-atoms, tetrabutylammonium cation (TBA) and disordered fluorine moieties are removed for structure clarity, CCDC: 2092373).

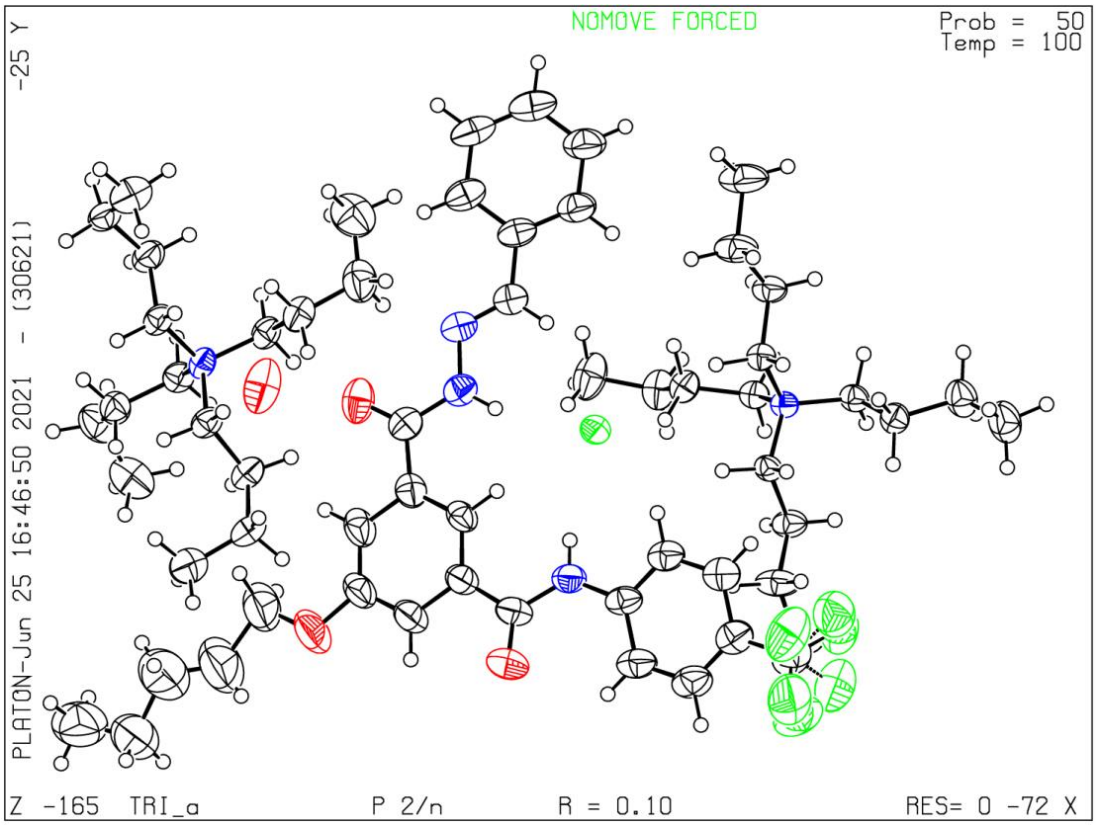

Figure S42. ORTEP diagram of **1d** co-crystalized TBACl. Ellipsoids are drawn at 50% probability.

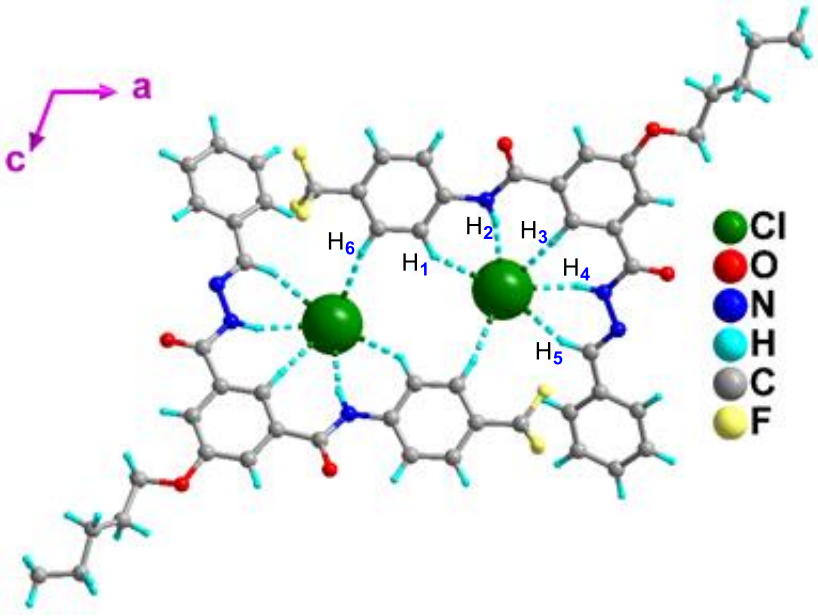

Figure S43. Hydrogen-bonded crystal structure of **1d** with Cl^- in 2:2 receptor:Cl^- binding mode (TBA cation moieties are removed for structure clarity).

X. NMR Spectra

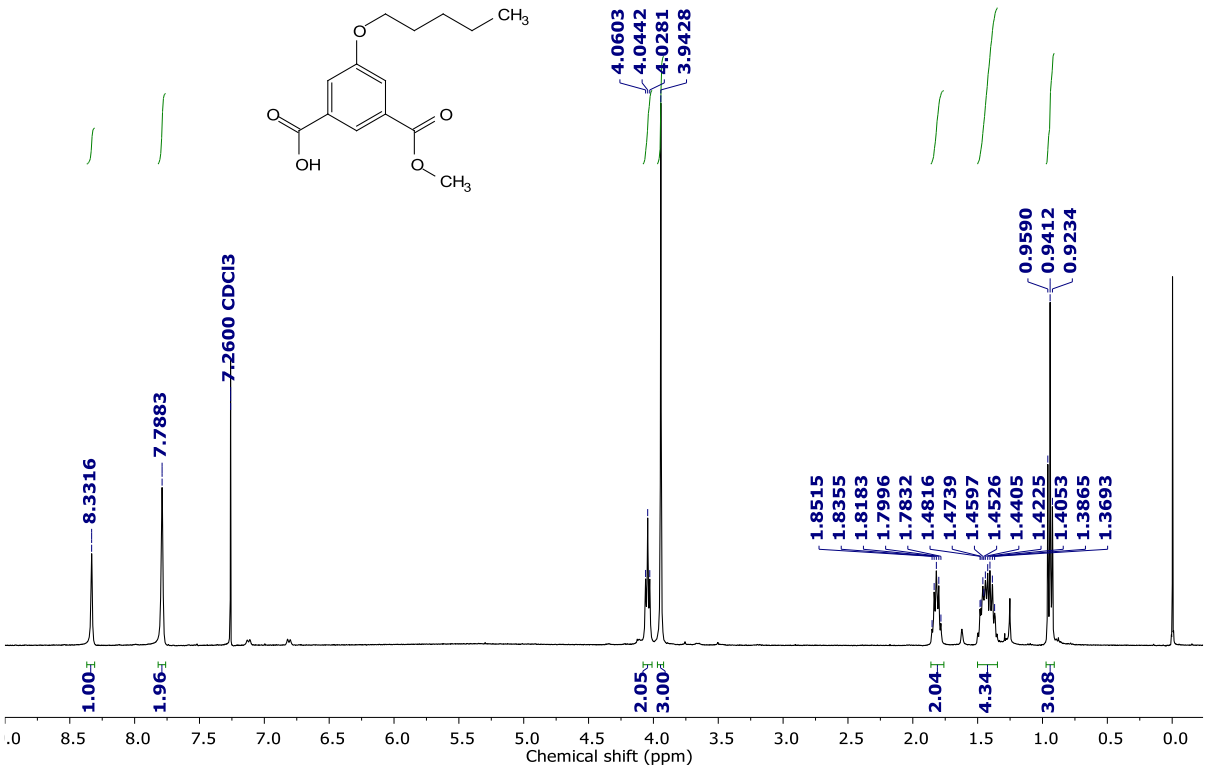

Figure S44. 400 MHz ^{1}H NMR spectrum of **3** in $CDCl_3$.

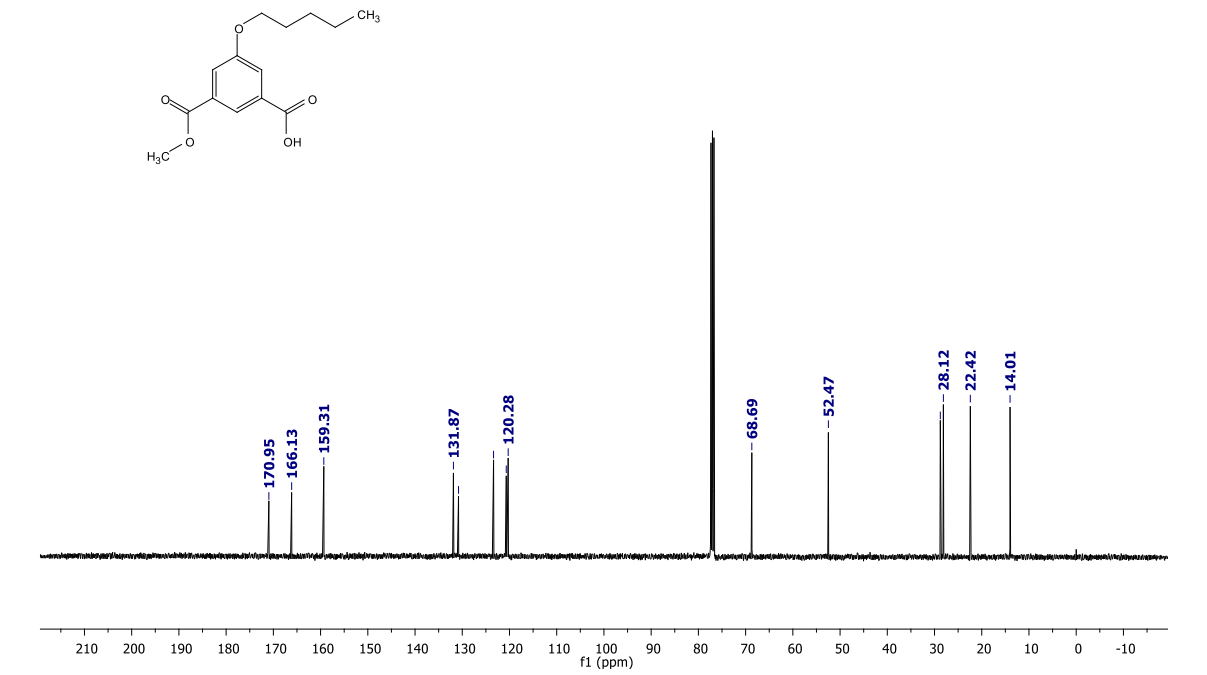

Figure S45. 101 MHz ^{13}C NMR spectrum of **3** in $CDCl_3$.

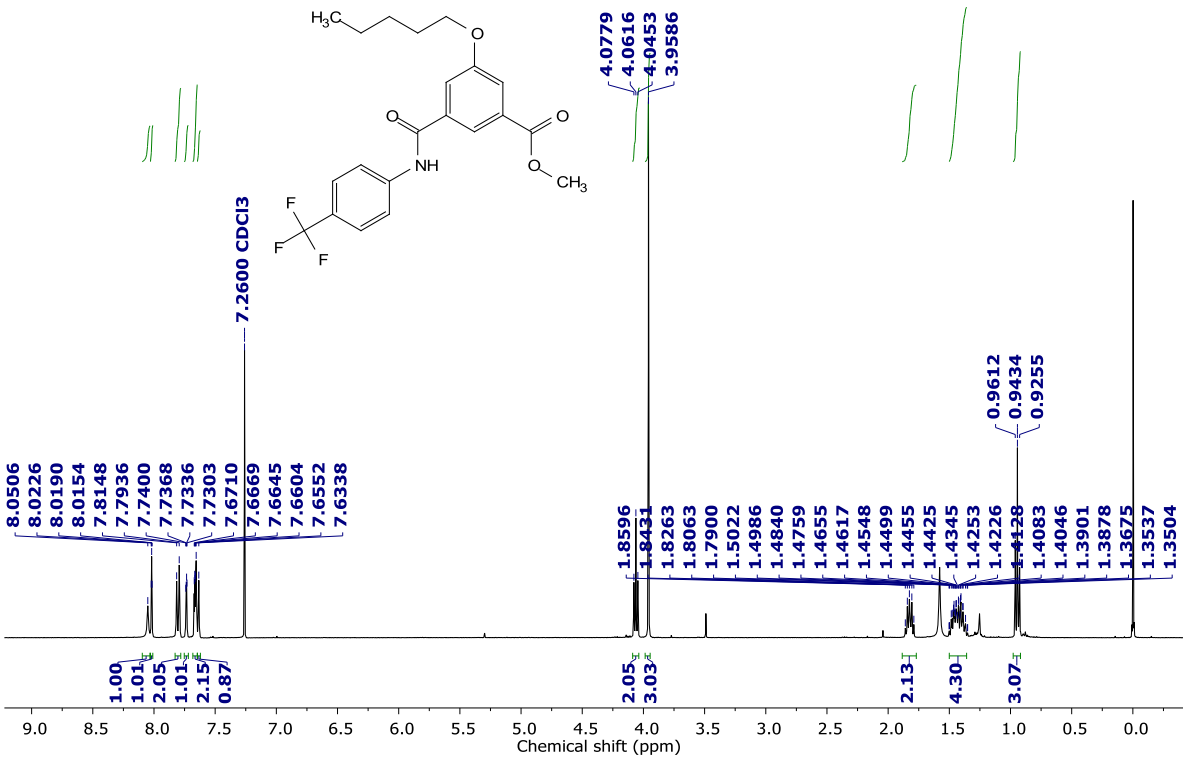

Figure S46. 400 MHz ^{1}H NMR spectrum of **4a** in $CDCl_3$.

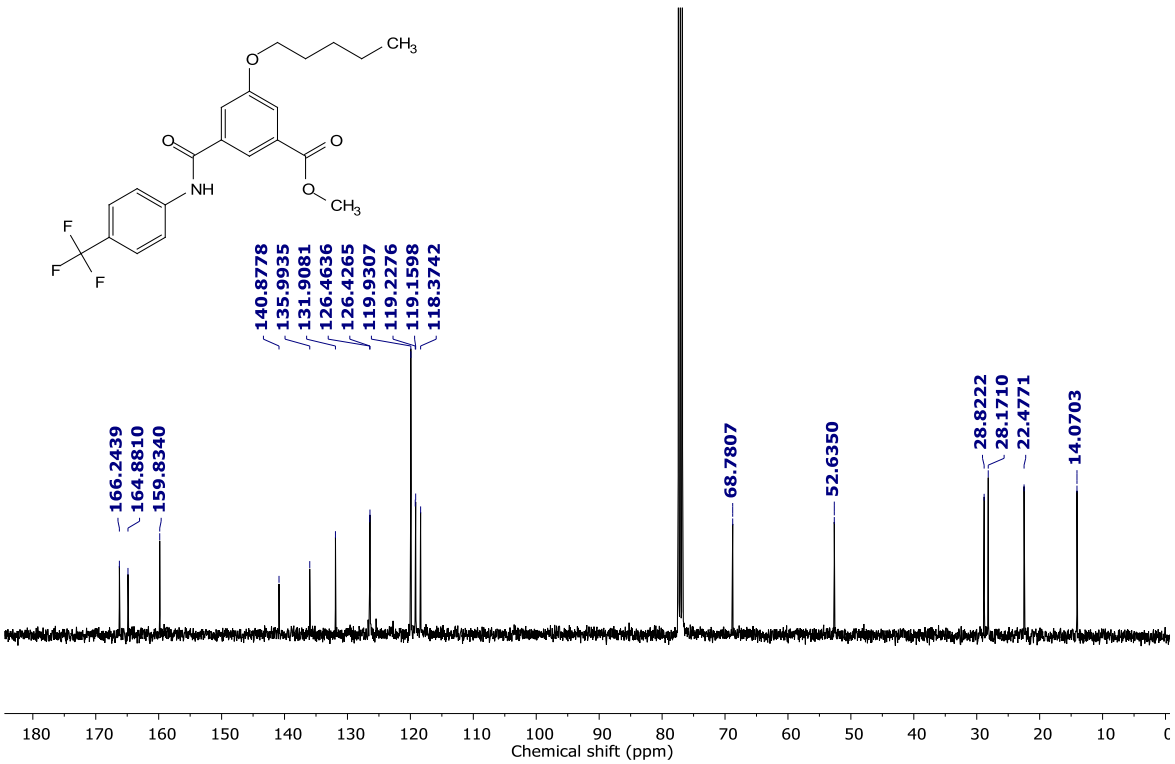

Figure S47. 101 MHz ^{13}C NMR spectrum of compound **4a** in $CDCl_3$.

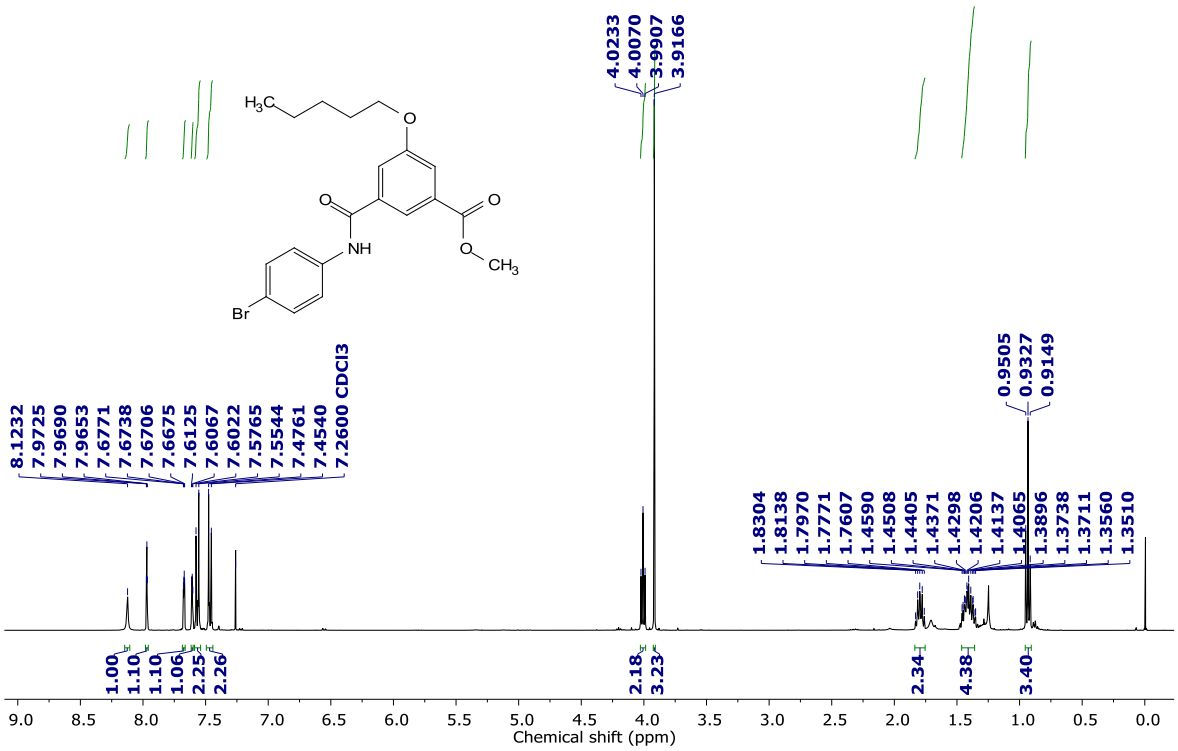

Figure S48. 400 MHz ^{1}H NMR spectrum of **4b** in $CDCl_3$.

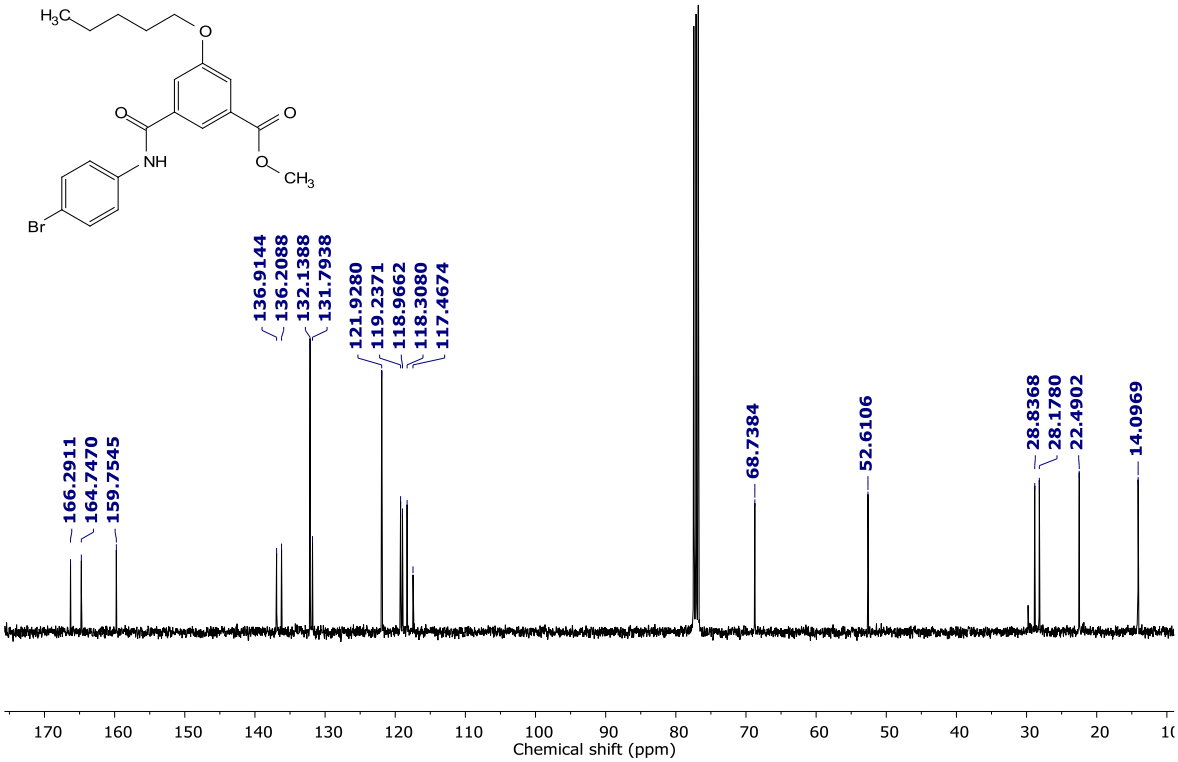

Figure S49. 101 MHz ^{13}C NMR spectrum of compound **4b** in $CDCl_3$.

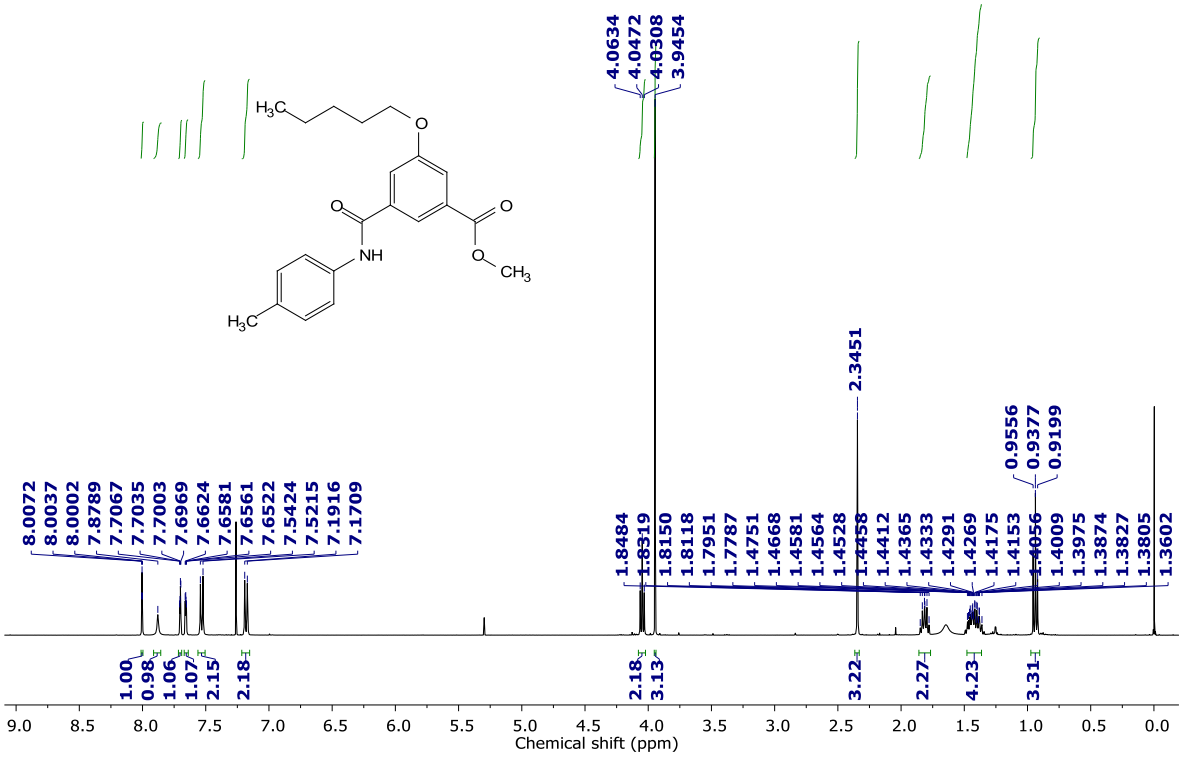

Figure S50. 400 MHz ^{1}H NMR spectrum of **4c** in $CDCl_3$.

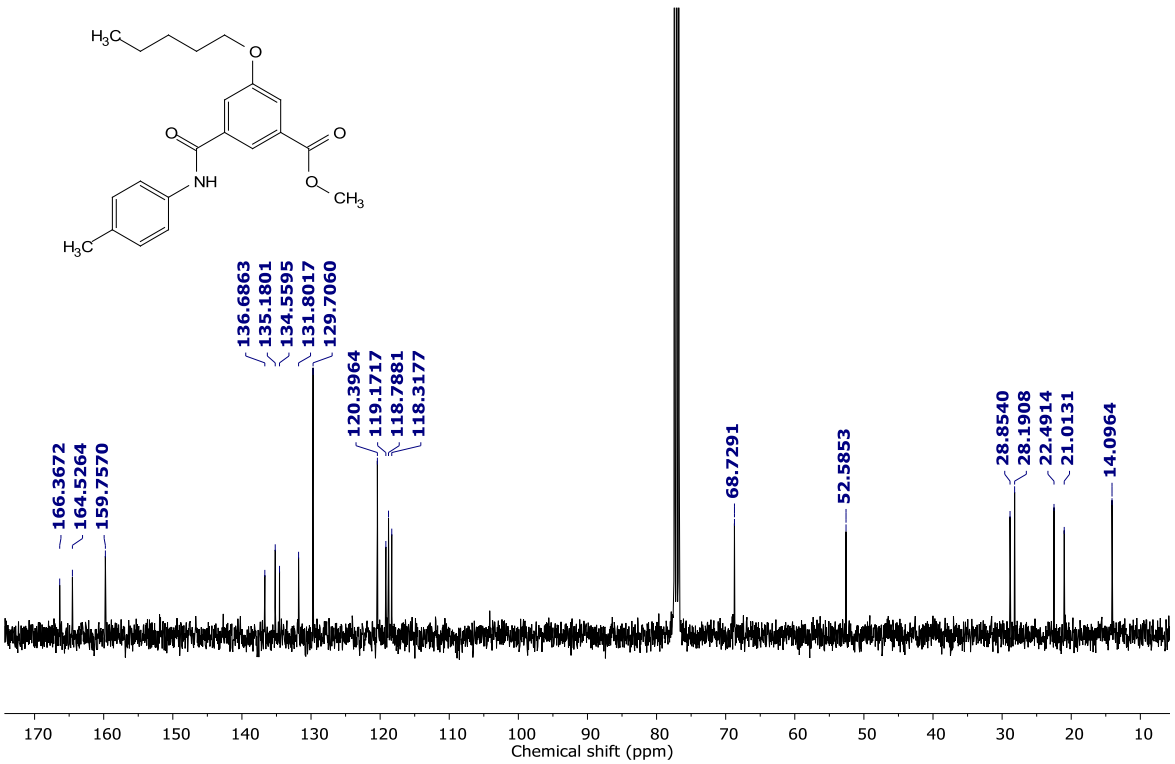

Figure S51. 101 MHz ^{13}C NMR spectrum of compound **4c** in $CDCl_3$.

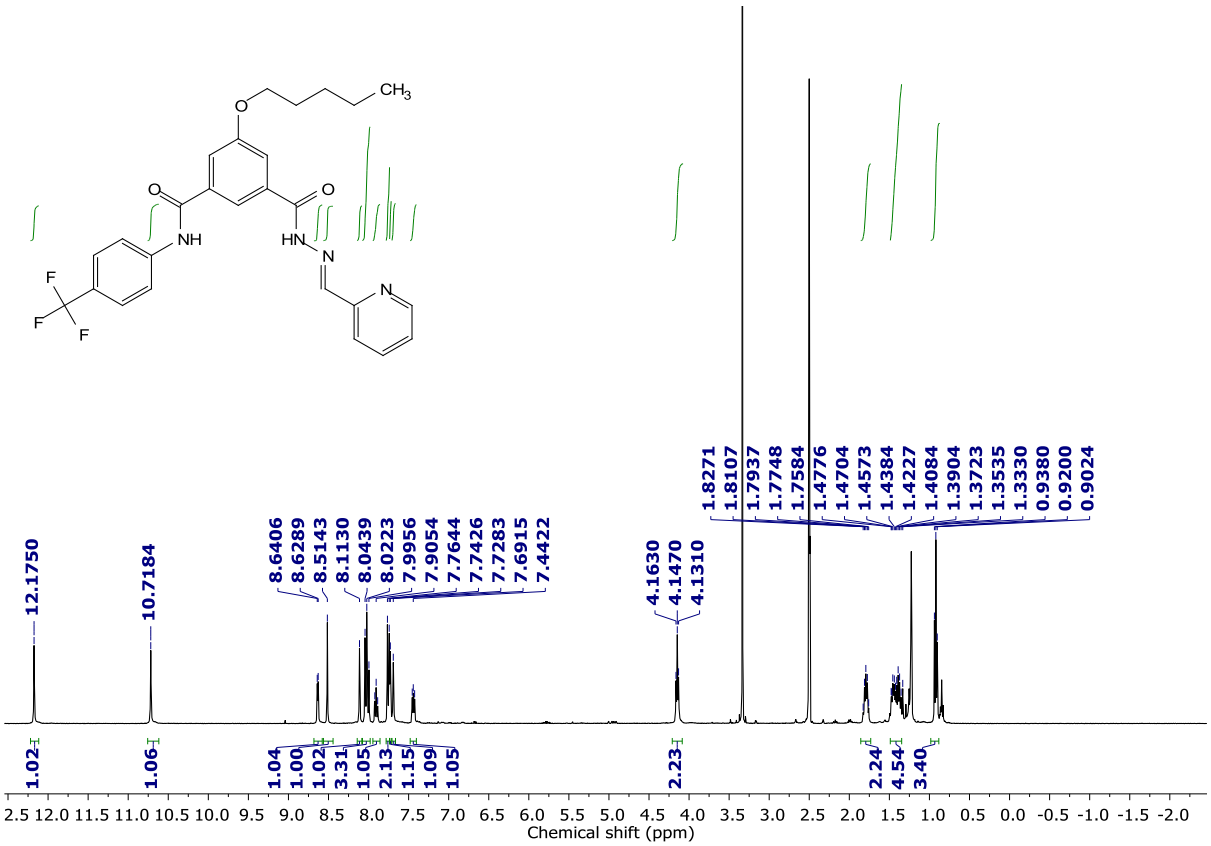

Figure S52. 400 MHz ^{1}H NMR spectrum of **1a** in DMSO-d_6.

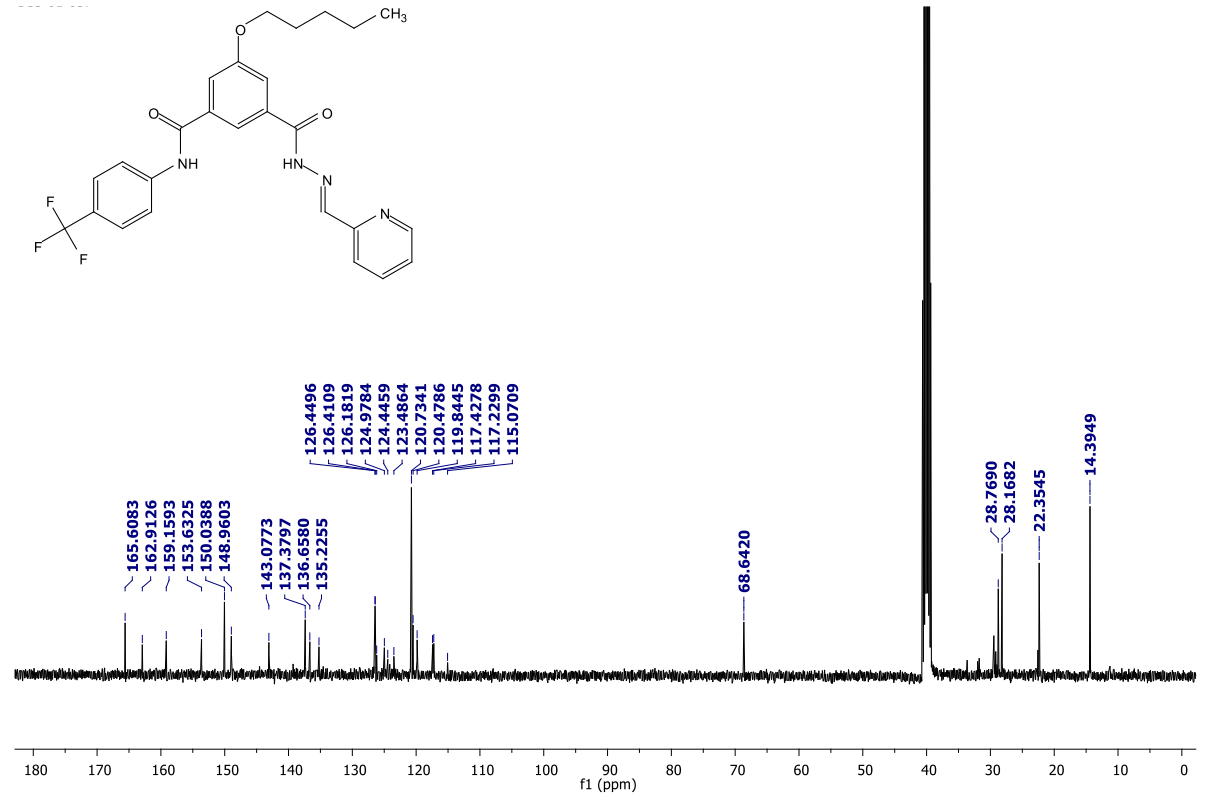

Figure S53. 101 MHz ^{13}C NMR spectrum of compound **1a** in DMSO-d_6.

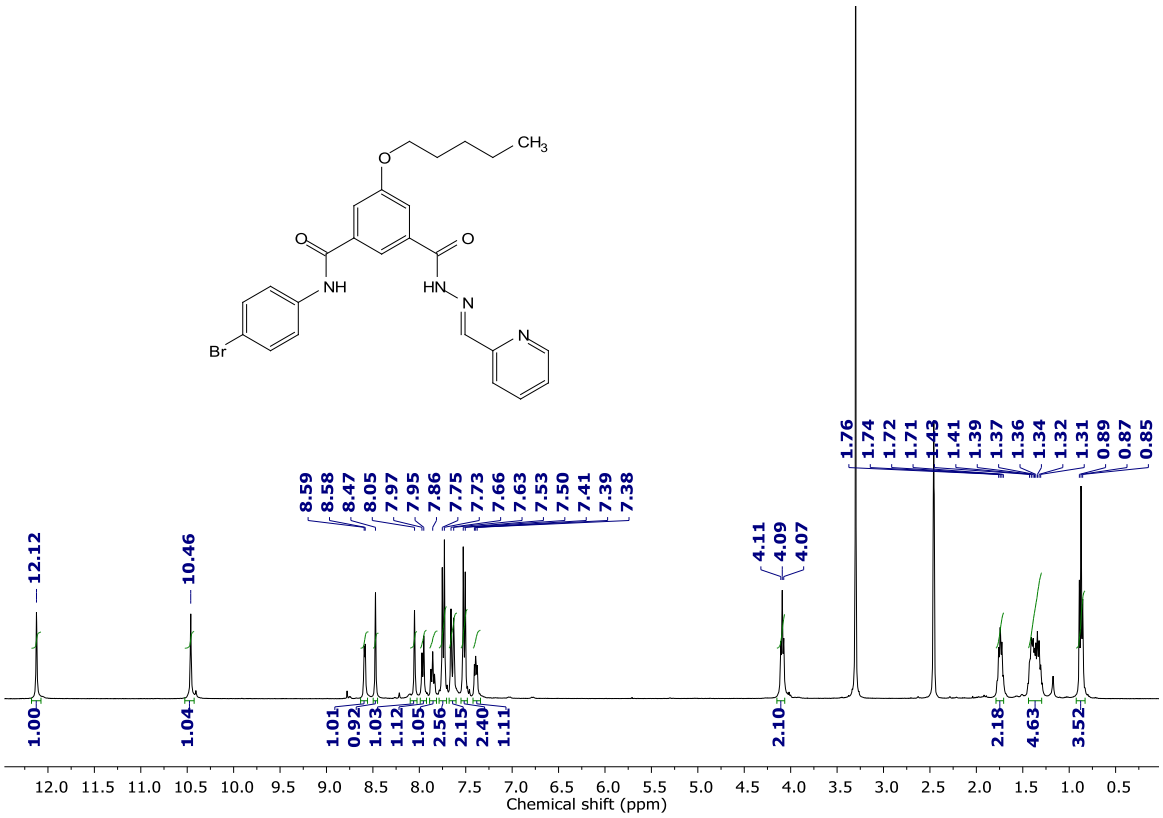

Figure S54. 400 MHz ^{1}H NMR spectrum of **1b** in DMSO-d_6.

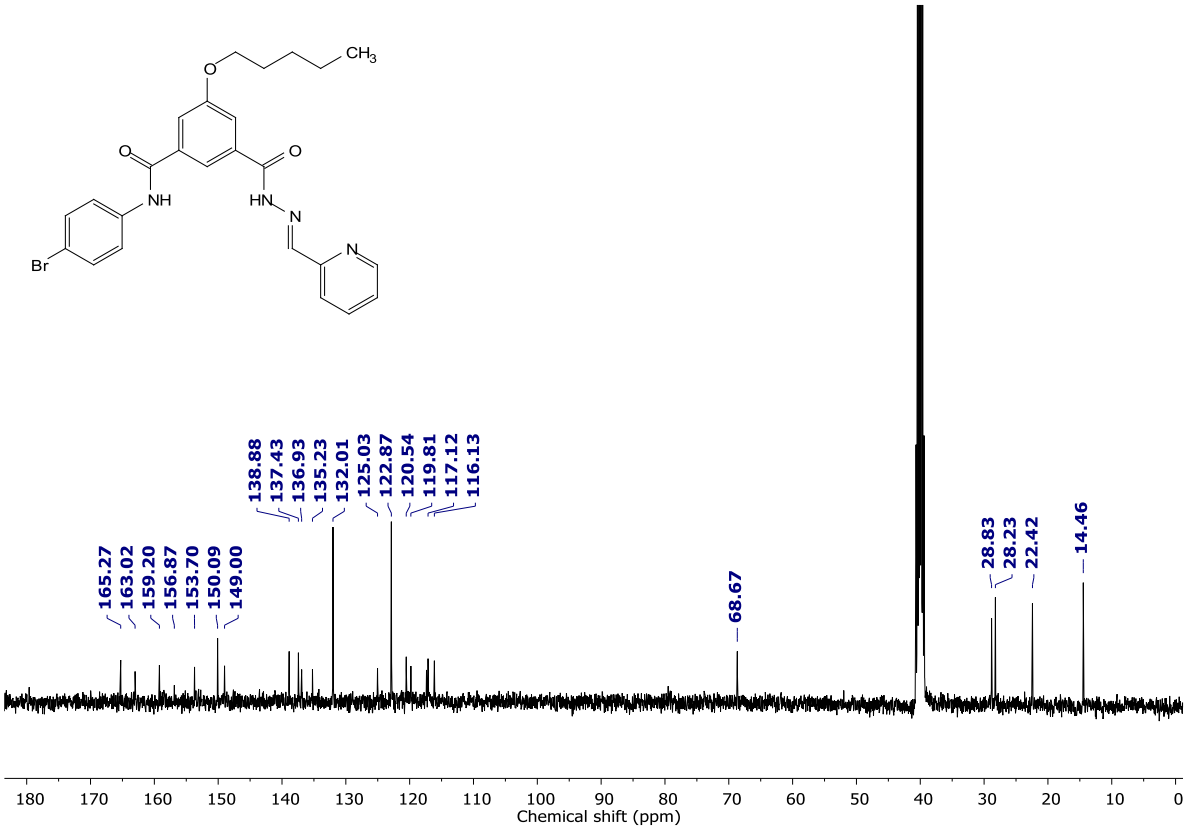

Figure S55. 101 MHz ^{13}C NMR spectrum of compound **1b** in DMSO-d_6.

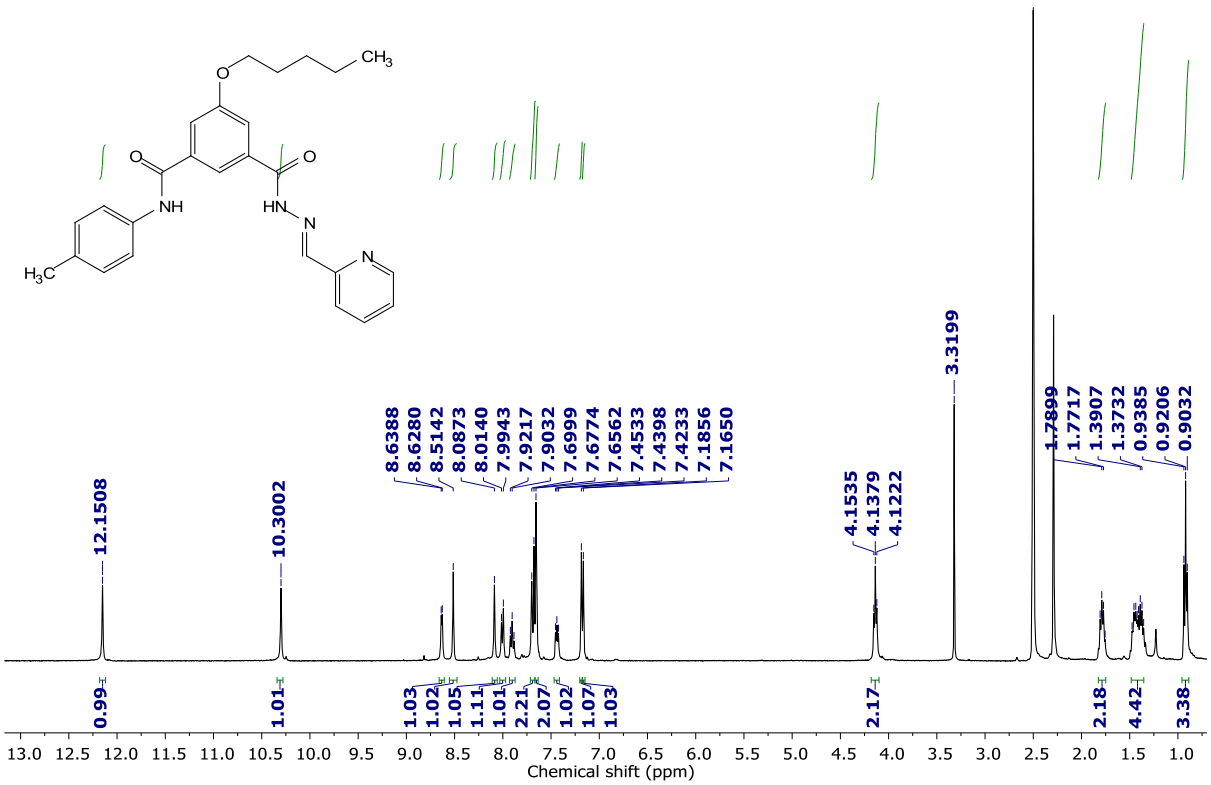

Figure S56. 400 MHz ^{1}H NMR spectrum of **1c** in DMSO-d_6.

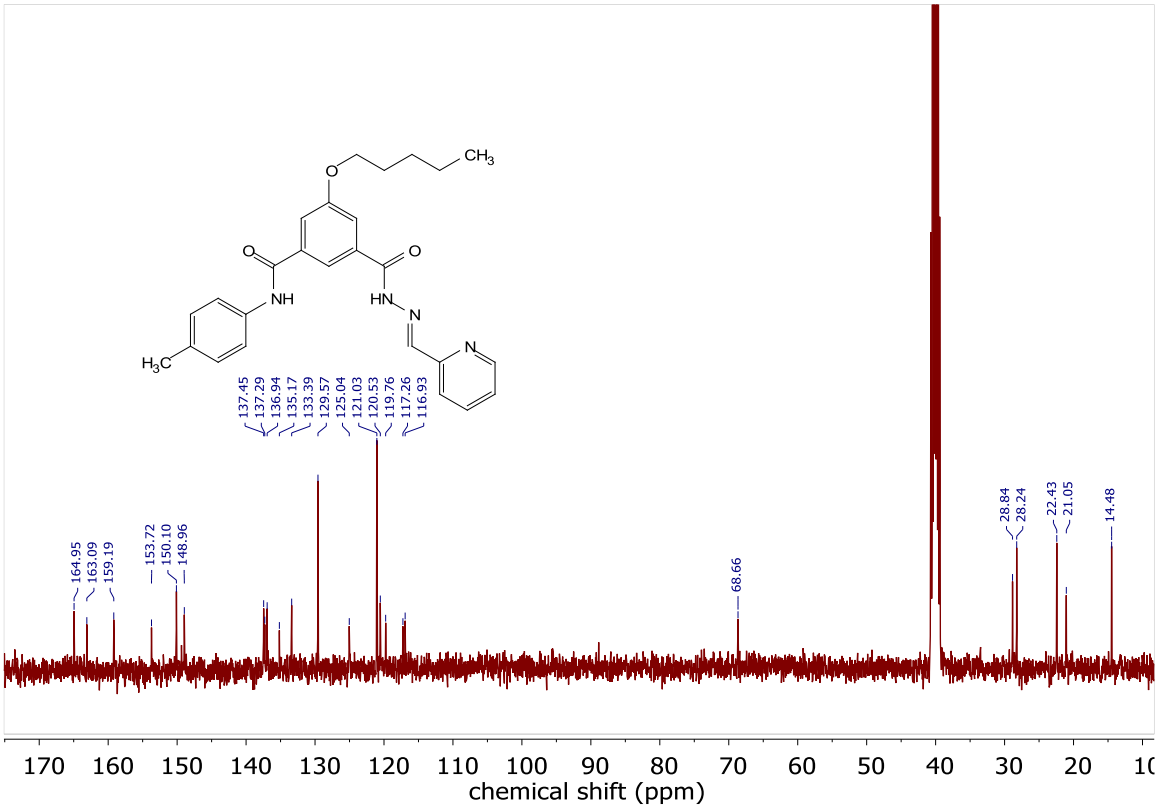

Figure S57. 101 MHz ^{13}C NMR spectrum of compound **1c** in DMSO-d_6.

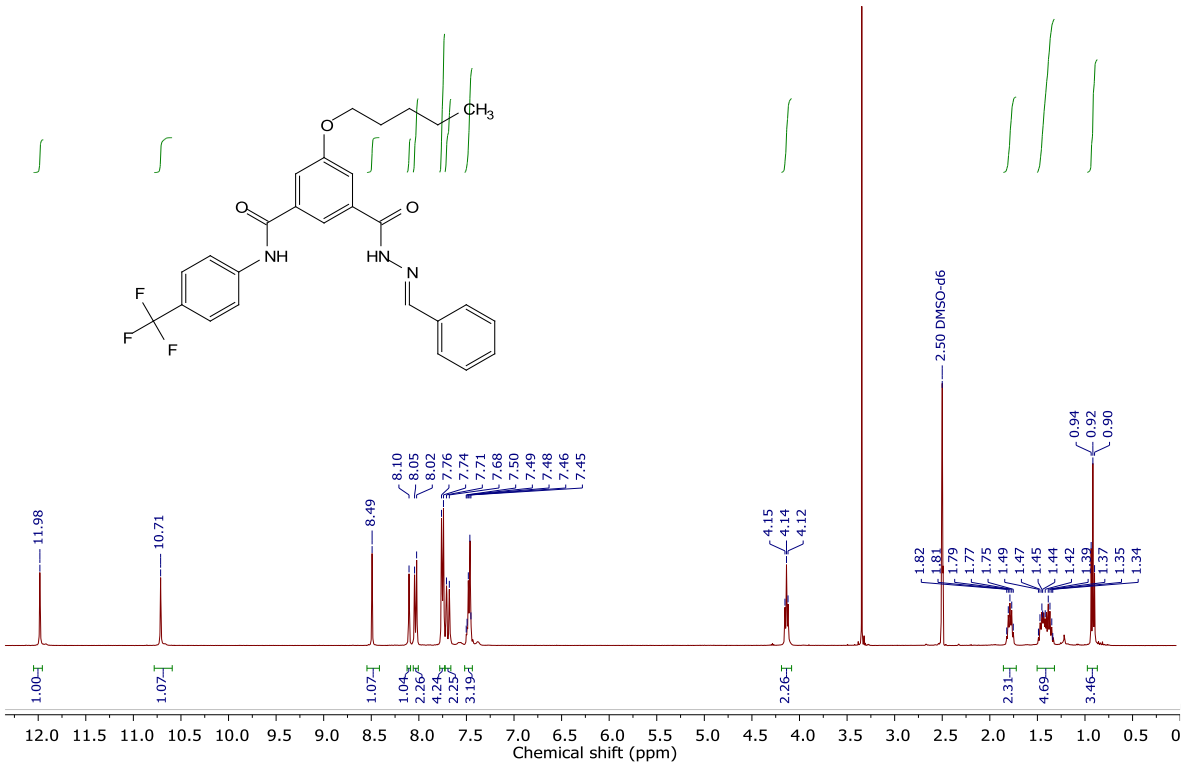

Figure S58. 400 MHz ^{1}H NMR spectrum of **1d** in DMSO-d_6.

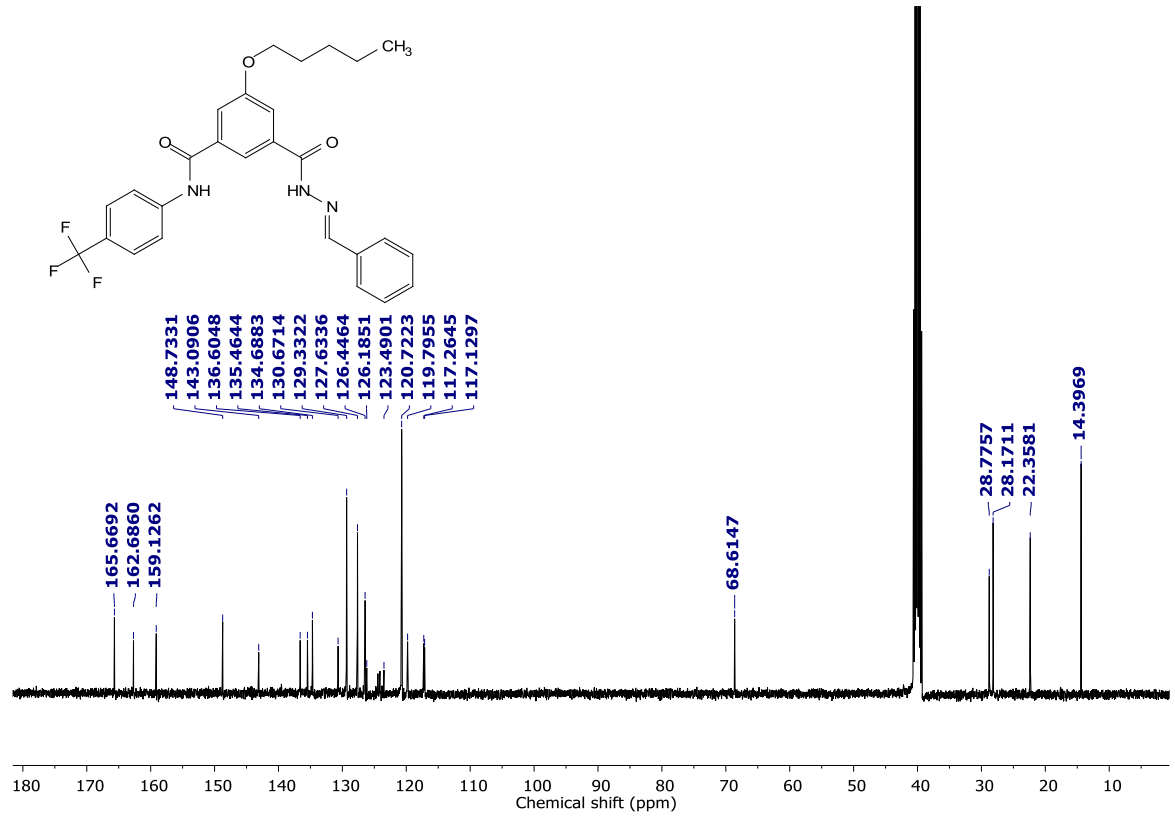

Figure S59. 101 MHz ^{13}C NMR spectrum of **1d** in DMSO-d_6.

XI. References:

S1. a) BindFit v0.5. http://app.supramolecular.org/bindfit/ (accessed on July 2017); b) P. Thordarson, *Chem. Soc. Rev.* **2011**, *40*, 1305–1323.

S2. a) Saha, T.; Dasari, S.; Tewari, D.; Prathap, A.; Sureshan, K. M.; Bera, A. K.; Mukherjee, A.; Talukdar, P. Hopping-Mediated Anion Transport through a Mannitol-Based Rosette Ion Channel. *J. Am. Chem. Soc.* **2014**, *136*, 14128−14135; b) Talukdar, P.; Bollot, G.; Mareda, J.; Sakai, N.; Matile, S. Synthetic Ion Channels with Rigid-Rod π-Stack Architecture that Open in Response to Charge-Transfer Complex Formation. *J. Am. Chem. Soc*. **2005**, *127*, 6528−6529; c) Gorteau, V.; Bollot, G.; Mareda, J.; Perez-Velasco, A.; Matile, S. Rigid Oligonaphthalenediimide Rods as Transmembrane Anion−π Slides. *J. Am. Chem. Soc.* **2006**, *128*, 14788−14789; d) Saha, T.; Hossain, M. S.; Saha, D.; Lahiri, M.; Talukdar, P. Chloride-Mediated Apoptosis-Inducing Activity of Bis(sulfonamide) Anionophores. *J. Am. Chem. Soc*. **2016**, *138*, 7558−7567.

S3. Vargas Jentzsch, A.; Emery, D.; Mareda, J.; Metrangolo, P.; Resnati, G.; Matile, S. Ditopic Ion Transport Systems: Anion–π Interactions and Halogen Bonds at Work. *Angew. Chem., Int. Ed.* **2011**, *50*, 11675−11678.

S4. Bhosale, S.; Matile, S. A simple method to identify supramolecules in action: Hill coefficients for exergonic self-assembly. *Chirality* **2006**, *18*, 849–856.

S5. Ren, C.; Ding, X.; Roy, A.; Shen, J.; Zhou, S.; Chen, F.; Yau Li, S. F.; Ren, H.; Yang, Y. Y.; Zeng, H. A halogen bond-mediated highly active artificial chloride channel with high anticancer activity. *Chem. Sci.* **2018**, *9*, 4044−4051.

S6. Sheldrick, G. A Short History of ShelX. *Acta crystallographica.* **2008**, *64*, 112−122.

S7. Spek, A. Structure validation in chemical crystallography. *Acta Crystallographica* **2009**, *65*, 148−155.